Environmental Science Nano

ROYAL SOCIETY OF CHEMISTRY

PAPER

View Article Online
View Journal | View Issue



Check for updates

Cite this: *Environ. Sci.: Nano*, 2026, **13**, 2092

# $Fe_3O_4$ nanozyme as a novel plant growth promoter for enhancing salt tolerance in cucumber seedlings: integrated analysis of growth physiology and transcriptional metabolism

Dan Xu, †[a] Bin Sheng,†[ab] Zhi-Hao Lin,[a] Xiao-Bin Wen,[ab] Xue-Ling Ye,*[b] Zhi-Yong Liu,[b] Ge Chen,[a] Jun Lv,[a] Dong-Hui Xu,*[a] Lin Qin,[a] Xiao-Min Xu[a] and Guang-Yang Liu *[a]

Received 20th October 2025,
Accepted 9th March 2026

DOI: 10.1039/d5en00970g

rsc.li/es-nano

Salt stress is one of the most significant factors limiting the output and quality of cucumber. The emergence of nanomaterials offers a new approach for overcoming the current limitations in non-biological stress management and achieving high-yield agriculture. Herein, we develop a PEG-modified $Fe_3O_4$ nanozyme (FNPs-G) and investigate its effect on the salt tolerance of cucumber seeds and seedlings. The results showed that FNPs-G significantly increased the germination rate by approximately 50% and promoted embryonic root growth (7.2% increase). Under salt stress, the foliar application of FNPs-G enhanced salt tolerance by increasing POD and CAT activities (38% and 17.4%, respectively), elevating proline (54.6%) and soluble sugar (3.13-fold) levels, and reducing $H_2O_2$ (24.6%) and MDA (33.8%) accumulation. The results of transcriptional and metabolic analyses indicate that the foliar application of FNPs-G can further mitigate salt stress in cucumber by enhancing phenylalanine metabolism, phenylpropanoid biosynthesis, and steroid biosynthesis. It also significantly facilitates tyrosine and arginine biosynthesis and upregulates the expression of genes encoding intracellular hydrolases and oxidoreductases, thereby maintaining cellular homeostasis. This study provides a theoretical and mechanistic basis for future investigations into the potential effects of FNPs-G during the fruiting stage and their influence on fruit quality under saline conditions.

### Environmental significance

Significant progress has been made in regulating plant metabolism and enhancing resistance to salt stress using FeO*x* nanoparticles, whose properties enable effective regulation of the intracellular redox state and scavenging of accumulated ROS in plants. In this study, PEG-modified $Fe_3O_4$ nanozyme (FNPs-G) were successfully synthesized. This modification not only reduced the particle size but also improved their dispersibility. This study confirmed that under salt stress conditions, FNPs-G also promote the growth and development of seedlings by enhancing the activity of antioxidant enzymes, reducing the levels of $H_2O_2$ and MDA, and effectively improving the salt tolerance of cucumber seedlings. These findings provide valuable insights into sustainable agricultural practices in saline–alkali environments.

## 1. Introduction

As one of the horticultural crops with the largest cultivation area in China's protected agriculture, cucumber holds significant economic value. However, the progressively worsening issue of soil salinization[1] poses a significant threat to the sustainable development of food and horticultural production in China and severely constrains the growth, development, and yield quality of cucumber.[2] Currently, the application of gene-editing technology to enhance stress tolerance shows significant promise. However, the lengthy research and development cycle, high costs, and concerns regarding the environmental and safety implications of genetically modified foods have collectively contributed to relatively sluggish progress in this area.[3,4] Therefore, it is urgent to develop critical strategies for improving agricultural productivity in salinized regions.

Reactive oxygen species (ROS) are by-products of plant aerobic metabolism. Salt stress can induce homeostatic imbalance in cucumber plants, leading to the substantial accumulation of ROS, which disrupts normal metabolic

[a] *State Key Laboratory of Vegetable Biobreeding, Institute of Vegetables and Flowers, Chinese Academy of Agricultural Sciences, Key Laboratory of Vegetables Quality and Safety Control, Ministry of Agriculture and Rural Affairs of China, Beijing 100081, China. E-mail: xudonghui@caas.cn, liuguangyang@caas.cn*
[b] *Horticulture College, Shenyang Agricultural University, Shenyang 110866, China. E-mail: yexueling@syau.edu.cn*
† Co-authors with equal contributions.

processes, causes oxidative damage to plant cells, and may even trigger programmed cell death, thereby significantly affecting the growth and development of cucumber.[5,6] Therefore, maintaining the homeostasis of ROS in plants is crucial for enhancing plant stress tolerance. Under these circumstances, nanomaterials (NMs) exhibit considerable potential for application in agricultural production and for mitigating oxidative damage induced by abiotic stresses.[7,8] This is attributed to their advantages such as low preparation cost, high catalytic activity, good environmental compatibility and the ability to simulate the function of antioxidant enzymes.[9] For instance, Lu *et al.*[10] applied synthesized $Mn_3O_4$ NPs to cucumber under salt stress conditions, which significantly enhanced the photosynthetic pigment content, net photosynthetic rate, and biomass accumulation in the cucumber leaves. Furthermore, oxidative stress in cucumber was effectively mitigated by strengthening the defense capability of endogenous antioxidants within the plants.

Nanozymes are a class of substances that integrate the characteristics of nanomaterials with catalytic functions. Compared to traditional enzyme catalysts, nanozymes exhibit remarkable advantages, including high stability and catalytic efficiency, low cost, and scalable production.[11,12] Moderate levels of Fe are conducive to the growth and development of cucumber plants. Additionally, Fe serves as a cofactor or activator for several key enzymes and proteins, playing a crucial role in maintaining redox homeostasis in plants.[13] Beyond its nutritional role, $Fe_3O_4$ nanoparticles possess a mixed-valence $Fe^{2+}/Fe^{3+}$ inverse spinel structure that enables rapid electron transfer through reversible redox cycling. This structural feature forms the physicochemical basis for their intrinsic peroxidase (POD)- and catalase (CAT)-like catalytic activities.[14] The $Fe^{2+}/Fe^{3+}$ redox couple facilitates electron donation and acceptance during $H_2O_2$ decomposition, allowing $Fe_3O_4$ nanoparticles to directly participate in ROS scavenging reactions rather than solely activating endogenous antioxidant enzymes.[15] Nano FeO*x* represents the first identified inorganic nanozyme with mimetic enzyme catalytic function. Its properties enable effective regulation of the intracellular redox state, scavenging of accumulated ROS within plants, and mitigation of cellular damage.[16] Since the initial discovery of $Fe_3O_4$ NPs with intrinsic POD and CAT activities in 2007, as well as their extensive validation and in-depth investigation, $Fe_3O_4$ NPs have effectively addressed the limitations of natural enzymes in practical applications. Moreover, their catalytic activity surpasses that of other FeO*x* nanoparticles, such as γ-$Fe_2O_3$ and α-$Fe_2O_3$.[17]

Despite the promising catalytic and nutritional properties of $Fe_3O_4$ nanoparticles, previous plant studies have primarily focused on physiological outcomes such as growth promotion and antioxidant enzyme activity enhancement, while the molecular regulatory mechanisms underlying nanoparticle-mediated salt tolerance remain poorly understood.[18] In addition, the effects of surface modification strategies, on nanoparticle stability, plant uptake, and enzymatic function under salt stress conditions have not been systematically investigated.[19,20] However, the agglomeration of $Fe_3O_4$ NPs (FNPs) not only diminishes their absorption and transport efficiency in plants but may also modify their enzymatic-like functional activities. Surfactants are a class of compounds characterized by a unique amphiphilic molecular structure. They modify the size, structure, and surface charge of $Fe_3O_4$ NPs *via* mechanisms such as adsorption or electrostatic interaction, thereby enhancing their dispersion and stability.[21] For instance, the modification of $Fe_3O_4$ NPs with polyethylene glycol (PEG) or polyethyleneimine (PEI) can substantially enhance their dispersion, stability, and biocompatibility in both aqueous and organic phases. This is critical for facilitating their transport and uptake in plants.[22,23] The understanding of $Fe_3O_4$-plant interactions remains in its infancy, and more comprehensive insight into the biological effects of $Fe_3O_4$ NPs on plants is essential for their future agricultural applications.

In this study, PEG-modified $Fe_3O_4$ nanozyme (FNPs-G) were successfully synthesized, and their synthesis process is illustrated in Scheme 1. The nanoparticles were systematically characterized to evaluate how surface engineering influences their catalytic behavior and biological performance. We compared different modification strategies and identified PEG as the optimal interfacial regulator for enhancing the stability and bioavailability of the nanoparticles. Using an integrated physiological, transcriptomic, and metabolomic framework, we further elucidated the coordinated regulation of phenylpropanoid biosynthesis, amino acid metabolism, and steroid biosynthesis pathways in response to FNPs-G under salt stress. These findings extend the current understanding of nanozyme–plant interactions beyond single-parameter physiological observations and provide mechanistic insight into how surface-engineered nanozymes function as redox modulators in crops.

## 2. Materials and methods

### 2.1. Materials

All chemical reagents used in this study were of analytical grade and used as received without any further purification. Ferrous chloride hexahydrate ($FeCl_3{\cdot}6H_2O$), ammonia (≥28%), and trisodium citrate (CA) were purchased from Shanghai McLean Biochemical Reagent Co., Ltd.; Ferric

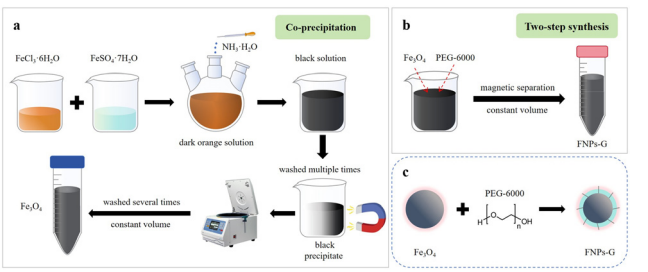


**Scheme 1** (a and b) Flow chart of the preparation of $Fe_3O_4$ and FNPs-G. (c) Schematic of FNPs-G.

sulfate heptahydrate ($FeSO_4{\cdot}7H_2O$) was purchased from Xilong Scientific Co., Ltd.; PEG-6000 was acquired from Shandong Keyuan Biochemistry Co., Ltd.; and sodium chloride (NaCl) and anhydrous ethanol were sourced from Sinopharm Chemical Reagent Co. Ltd. The kits for determining physiological and biochemical indices, including root vigor, superoxide dismutase (SOD), peroxidase (POD), catalase (CAT), glutathione (GSH), hydrogen peroxide ($H_2O_2$), total antioxidant capacity (T-AOC), proline (Pro), malondialdehyde (MDA), and soluble sugar, and phosphate-buffered saline (PBS) tablets were purchased from Beijing Solarbio Technology Co., Ltd. Deionized water was prepared using a laboratory ultrapure water system (model Milli-Q Advanta). The cucumber variety 'Zhongnong 18' was provided by the Institute of Vegetable and Flower Research, Chinese Academy of Agricultural Sciences (CAAS).

### 2.2. Preparation of FNPs-G nanozyme

The synthesis of magnetite FNPs was carried out using a modified chemical co-precipitation method, following the procedure described in previous studies.[24] Briefly, 1.2 g of $FeCl_3{\cdot}6H_2O$ and 0.7 g of $FeSO_4{\cdot}7H_2O$ were dissolved in 10 mL of deionized water and subsequently mixed thoroughly by ultrasonication. The resulting solution was filtered through a 0.22 μm filter membrane and diluted with 240 mL of deionized water. Under magnetic stirring at 80 °C for 30 min, 10 mL of ammonia was added dropwise. After an additional 15 min of stirring, 0.1 g of CA was introduced, and the reaction was terminated for 30 min. The mixture was cooled to room temperature, magnetically separated, and repeatedly washed with ethanol and deionized water to remove residual salts. Large aggregates were eliminated by centrifugation at 9000 rpm for 10 min (repeated several times), and the final product was resuspended in 30 mL of deionized water.

Next, the FNPs were coated with PEG-6000. Specifically, 10 g of PEG-6000 was dissolved in 100 mL of deionized water and magnetically stirred at 60 °C for 30 min. The pre-synthesized FNPs were added and stirred for 10 min, and the large particles were removed by magnetic separation several times and fixed in 30 mL with deionized water. Scheme 1c illustrates the mechanism of coating PEG-6000 on the surface of the FNPs. Finally, the mass concentration of FNPs and FNPs-G in 1 mL of suspension was calculated.

### 2.3. Characterization

The size and morphology of the nanoparticles were characterized by scanning electron microscopy (SEM, SM-6300, Japan) and transmission electron microscopy (TEM, JEM1200EX, Japan). Their hydrodynamic diameters and zeta potentials were measured using a nanoparticle sizer. Qualitative and quantitative information on the molecular functionality of FNPs, including intramolecular functional group details, was obtained *via* Fourier-transform infrared spectroscopy (FTIR, Nicolet iS10, USA). Structural and morphological information of $Fe_3O_4$ NPs was determined using an X-ray diffractometer (Bruker D8 Advance, Germany), which exploits the diffraction interaction between X-rays and crystalline materials. The magnetic properties of the solid samples were evaluated under an external magnetic field of ±10 kOe using a vibrating sample magnetometer (VSM) system integrated with a superconducting quantum interference device (SQUID-VSM, MPMS-3, USA).

### 2.4. Experimental treatment

Seed soaking treatment: Based on previous experience, cucumber seeds were subjected to FNPs-G treatments at concentrations of 50 mg $mL^{-1}$, 100 mg $mL^{-1}$, and 200 mg $mL^{-1}$. Specifically, 25 seeds were placed in a petri dish containing 6 mL of the treatment suspension. For the control group, deionized water was used as a substitute for the FNPs-G suspension. The petri dishes were incubated in a thermostatic shaker maintained at 25 °C and 100 rpm for 24 h. Following the incubation period, the treated seeds were thoroughly washed three times with deionized water to remove residual FNPs-G. Subsequently, the moistened seeds were evenly distributed on filter paper in a germination box and transferred to a constant-temperature light incubator (25 °C ± 1 °C) under dark conditions for 5 days. Deionized water (1–2 mL) was replenished every 24 h to maintain humidity.

Foliar spraying treatment: A concentration of 50 mg $mL^{-1}$ FNPs-G was employed as the treatment condition for foliar spraying. A salt concentration of 100 mM was selected for stress treatment, consistent with the majority of experimental studies investigating the effects of salt stress on plant growth.[25] Preliminary salt concentration gradient experiments confirmed that 100 mM NaCl represents a moderate stress level for cucumber seedlings (Table S2, SI). Cucumber seedlings were cultivated using the slant plate nursery method, as detailed in the experimental protocol.[26] Upon cotyledon unfolding, healthy and uniformly growing seedlings were selected and transplanted into 6-well black hydroponic boxes. The seedlings were subsequently grown in a 1/2-strength Hoagland's nutrient solution until they reached the two-leaf-one-heart stage. Once the cucumber plants reached the three-leaf-one-heart stage, they were subjected to NaCl stress treatment. Tap water without NaCl was used as the control treatment. Subsequently, different foliar spray treatment solutions were formulated as follows: (1) a control solution consisting of deionized water containing 0.02% Tween 20 and (2) an FNPs-G treatment solution containing 50 mg $mL^{-1}$ FNPs-G with 0.02% Tween 20. Cucumber seedlings subjected to NaCl stress were acclimatized under low-light conditions for 3–4 h before being foliar-sprayed with the FNPs-G treatment. Specific procedures: the control solution and FNPs-G solution were separately loaded into spray bottles. During spraying, the foliage was uniformly moistened by applying the solutions using the spray bottles. Under light conditions, the solution was sprayed onto the underside of cucumber leaves until it dripped off. Foliar spraying was performed once daily for 5 consecutive days.

 

### 2.5. Quantitative analysis of Fe content in cucumber endosperm

To estimate the extent of $Fe_3O_4$ uptake, twenty cucumber seeds were treated with 200 mg $mL^{-1}$ FNPs and FNPs-G for 24 h and washed and subsequently dissected to separate the seed coat from the endosperm using a razor blade. The endosperm was ground in liquid nitrogen and transferred to a nitrification tube, where it was digested by adding 6 mL of concentrated nitric acid and incubated at 95 °C for 2 h. The resulting solution was diluted with deionized water and adjusted to a final volume of 25 mL. The Fe content in the samples was quantified using an inductively coupled plasma optical emission spectrometer (ICP-OES).

### 2.6. Magnetic resonance imaging (MRI) of cucumber seeds

MRI tests were performed in the Magnetic Resonance Laboratory of the Center for Analysis and Testing at Tsinghua University. Treated and control seeds were loaded into identical MRI tubes (at least 20 seeds per treatment) and examined simultaneously to minimize potential instrumental variability and to emphasize differences attributable to the presence of NPs. The seeds were dissected into seed coat and endosperm using a razor blade. A sponge sheet was used to physically separate the treated and control seeds. The control seeds were marked with one corner removed for easy differentiation during analysis.

### 2.7. Germination analysis and plant growth assessment

Seeds treated with varying concentrations of FNPs-G were uniformly placed in germination cassettes containing two layers of filter paper and grown under dark conditions for 5 days to evaluate the exposure of embryonic roots and germination performance. Germination was recorded when the radicle length equaled the seed length, with counts beginning on the second day. Photographs were taken daily for 5 consecutive days. To evaluate root elongation in cucumber seedlings following FNPs-G treatment, images of 5-day-old seedlings grown on an inclined plate were captured.

The height of the cucumber plants was measured with a ruler. Representative leaves were excised using scissors, and leaf images were captured using a leaf scanner. The total leaf area was subsequently determined using a leaf analysis system. Fresh and dry weights of the leaves were measured using an electronic balance. The representative cucumber leaves were collected, placed in aluminum foil bags, rapidly frozen in liquid nitrogen for 5 minutes, and subsequently stored at −80 °C for subsequent analysis.

### 2.8. Quantitative determination of nutrient element concentrations in cucumber leaves

Fresh cucumber leaves were excised and thoroughly rinsed to remove residual dust and the treatment solution from their surfaces. After blotting dry with filter paper and measuring their fresh weight, the leaves were transferred to a nitrification tube, followed by the addition of 6 mL of concentrated nitric acid for digestion. The tubes were incubated at 95 °C for 2 h. The resulting digest was diluted with deionized water and adjusted to a final volume of 25 mL. The ICP-OES instrument was calibrated using standard solutions, and the signal intensities of the elements were recorded. A standard curve was constructed based on the relationship between absorption intensity and concentration of the standard solutions. Using this calibration curve, the recorded absorption intensities of the samples were converted into the corresponding elemental concentrations. Based on these calculations, the content of metal elements in the cucumber leaves was determined. Each treatment group was replicated three times, and the data were subjected to statistical analysis.

### 2.9. Methods for determining physiological indicators in cucumber

Root vigor, $H_2O_2$ content, SOD activity, POD activity, CAT activity, GSH content, MDA content, Pro content, and soluble sugar content of cucumber seedlings were measured using a micro-assay method. The assay kits were procured from Beijing Solarbio Technology Co., Ltd., and all operations were conducted strictly in accordance with the manufacturer's instructions. Absorbance values were measured using a microplate reader, and the content values for each index were calculated based on the sample mass formula provided for 96-well plate assays.

### 2.10. Transcriptomic and metabolomic analyses of FNPs-G-regulated salt tolerance in cucumber

The second true leaves of cucumber in both the control and treatment groups were wrapped in aluminum foil, snap-frozen in liquid nitrogen, and subsequently transferred to a sealed bag. A total of 16 samples, representing four different treatments, were then shipped to Wuhan Maiwei Metabolic Biotechnology Co., Ltd. for further analysis. The specific assay methods for transcriptome and metabolome analyses are provided in the SI.

Transcriptomic sequencing was performed on the leaves of cucumber seedlings to identify functions of Gene Ontology (GO) terms and Kyoto Encyclopedia of Genes and Genomes (KEGG) pathways enriched and annotated by differentially expressed genes (DEGs). Non-targeted metabolomics analysis was employed to screen for differential metabolites (DAMs) and annotate the associated KEGG pathways. Through integrative analysis of transcriptomics and metabolomics data, key metabolic pathways and critical genes were identified, with the aim of elucidating the molecular mechanisms underlying the response of FNPs-G to salt stress in cucumber plants.

### 2.11. Statistics and reproducibility

All the above-mentioned experiments were conducted with three replicates to minimize errors. The data were

summarized and analyzed using Excel, and the significance of differences was evaluated by one-way ANOVA using SPSS software.

## 3. Result

### 3.1. Characterization of $Fe_3O_4$ nanozyme

Owing to the magnetic dipole interactions and van der Waals forces of the magnetic nanoparticles,[27] SEM and TEM analyses revealed that both FNPs and FNPs-G exhibited uniform sizes, spherical morphologies, and good stability with diameters ranging from 15 to 20 nm. In aqueous solutions, these particles aggregated into clusters (Fig. 1a and b, respectively). PEG can form a protective layer on the surface of NPs, effectively preventing their aggregation. As clearly demonstrated in Fig. 1c and d, PEG-modification of FNPs significantly reduced the hydrodynamic diameter and altered the surface chemistry of the particles. Additionally, preliminary experiments confirmed the POD-like activity of the prepared FNPs and FNPs-G (Fig. S1). Comprehensive physicochemical characterization data, including hydrodynamic diameter, zeta potential, and UV-vis spectra of FNPs modified with CA, PEG, PEI, and CTAB, are presented in Fig. S7–S14 (SI).

FTIR spectroscopy was employed to identify the functional groups of the materials, and several characteristic absorption peaks were observed in the obtained spectra (Fig. 1e). Both FNPs and FNPs-G exhibited an Fe–O bond absorption peak at 577 $cm^{-1}$, corresponding to the vibrational mode of $Fe^{3+}$–O in the tetrahedral position. The absorption peak near 1400 $cm^{-1}$ is typically associated with the bending vibration of the ether bond (C–O–C) in the PEG molecule and constitutes part of the characteristic PEG peaks, confirming the successful surface modification of $Fe_3O_4$ NPs with PEG. The intensity of the C=O absorption peak for FNPs-G was significantly reduced in the range of 1620–1630 $cm^{-1}$, indicating the interaction between $Fe_3O_4$ NPs and PEG.[28] The absorption peak near 3400 $cm^{-1}$ corresponds to the stretching vibration of the O–H group, which reflects the hydrophilic nature and ease of binding of PEG. The weak absorption peak at 2877 $cm^{-1}$ is attributed to the vibration of the C–H group.[29] The presence of the C–H group is due to binding between FNPs and $CO_2$-free molecules in the atmosphere, suggesting the surface modification of FNPs by PEG-6000.

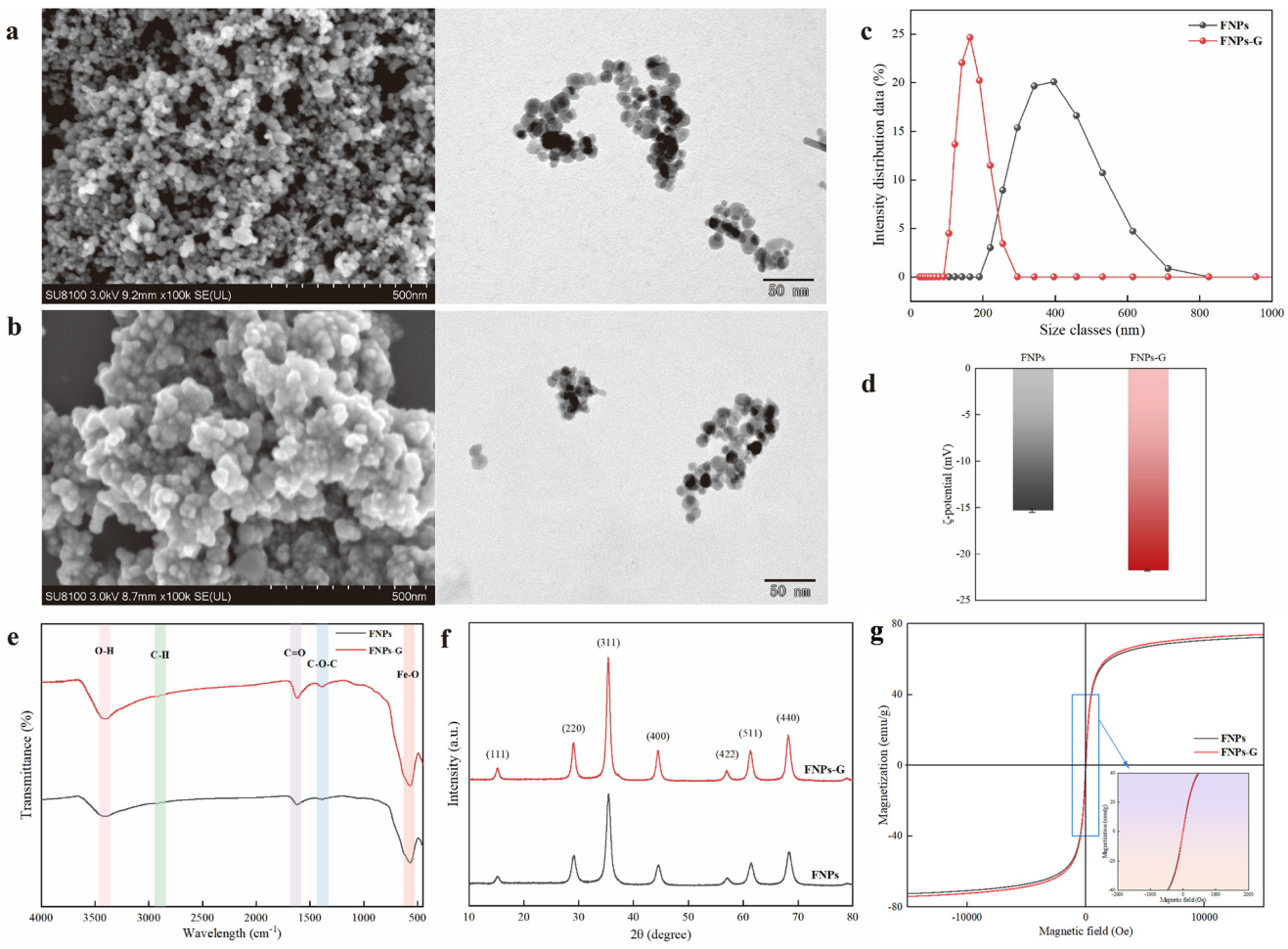


Fig. 1 Characterization of $Fe_3O_4$ NPs. (a and b) SEM and TEM images of FNPs and FNPs-G. (c and d) Hydrodynamic diameter and ζ-potential characterization of FNPs and FNPs-G. (e and g) FTIR, XRD and VSM characterization of FNPs and FNPs-G.

 

The XRD results (Fig. 1f) confirm that the prepared material exhibits a single-phase cubic spinel structure, indicating a stable crystal lattice with no detectable impurity phases. The positions and relative intensities of the diffraction peaks are consistent with the standard XRD database for magnetite ($Fe_3O_4$). Based on JCPDS No. 19-0629, the planar indices are expressed as (111), (220), (311), (400), (422), (511) and (440).[30] However, the diffraction peak angles exhibit a slight shift, probably because the interaction of PEG in the process for the modification of $Fe_3O_4$ may introduce stresses and strains on the surface of the particles. This phenomenon may result in a reduction in grain size. According to Bragg's law, a decrease in grain size leads to an increase in interplanar spacing, causing the diffraction peaks to shift toward higher $2\theta$ angles.

We further evaluated the magnetic properties of the samples at room temperature. As depicted in Fig. 1g, the curves confirm that both FNPs and FNPs-G exhibit superparamagnetic behavior. Specifically, in the absence of an external magnetic field, the net magnetic moment is zero, while under an applied magnetic field, the magnetic moments rapidly align, resulting in high initial permeability and specific saturation magnetization. Additionally, it can be seen that all the samples are categorized as soft magnetic. This is due to the fact that the resulting hysteresis curves have a narrow region (coercivity $<$132 Oe) and a symmetrical reverse sequence when subjected to an external magnetic field.[31]

### 3.2. Surface interactions and uptake of $Fe_3O_4$ nanozyme in cucumber seeds

To investigate the effects of FNPs on the structure of cucumber seed coats and their internalization, we conducted SEM analyses after treating the seeds with two different suspensions for 24 h. The results revealed that $Fe_3O_4$ significantly altered the epidermal structure of the seed coat (Fig. 2). SEM images demonstrated that the surface of the cucumber seed coat transitioned from smooth to spiculated following treatment with FNPs. Additionally, notable changes were observed in the cell wall morphology. Notably, FNPs-G induced fewer alterations in the seed coat and cell walls compared to the unmodified FNPs, providing strong evidence of their enhanced biocompatibility and reduced cytotoxicity. Furthermore, FNPs were detected on the endosperm of the cucumber seeds, with partial penetration and dispersion observed in the endosperm of the FNPs-G-treated seeds (Fig. 2g and k, respectively), suggesting improved absorption and utilization of FNPs-G by the plant. It is reasonable to hypothesize that the physical interaction between the seeds and nanoparticles may modify the permeability of the seed coat, thereby potentially influencing the water uptake kinetics during the early stages of germination.

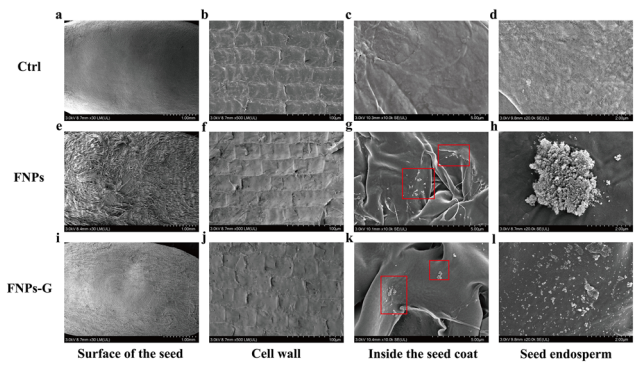


Fig. 2 Scanning electron micrographs of untreated seeds (a–d) and seeds treated with 200 mg $mL^{-1}$ FNPs (e–h) and FNPs-G (i–l) for 24 h. Seed surface, cell wall, inner seed coat, and seed endosperm, from left to right. Scale bars: (a, e, i) 1 mm; (b, f, j) 100 μm; (c, g, k) 5 μm; and (d, h, l) 2 μm.

To quantitatively evaluate the internalization of FNPs into the endosperm of cucumber seeds following FNPs and FNPs-G seed-soaking treatments, we performed ICP-OES analysis to determine the iron content. For this purpose, seeds treated with 200 mg $mL^{-1}$ FNPs and FNPs-G for 24 h, as well as untreated control seeds, were digested and analyzed by ICP-OES. The iron content was determined to be 114.87 ± 0.6 mg $kg^{-1}$ in the control group, 114.37 ± 1.0 mg $kg^{-1}$ in the 200 mg $mL^{-1}$ FNPs-treated group, and 131.63 ± 1.3 mg $kg^{-1}$ in the 200 mg $mL^{-1}$ FNPs-G-treated group. These results demonstrate that PEG surface modification significantly enhances the dispersion and biocompatibility of FNPs in solution, thereby promoting their sustained uptake by cucumber seeds.

### 3.3. MRI of cucumber seeds

Representative two-dimensional axial slices of cucumber seeds treated with FNPs and FNPs-G were visualized using magnetic resonance imaging (MRI) for independent analysis of their absorption (Fig. 3). Subsequently, a comprehensive evaluation of the proton spin–spin relaxation time ($T_2$) was conducted. The images indicate that the presence of FNPs substantially modifies the chemical environment within the seeds, which is attributed to the magnetic properties of iron. This shortened relaxation time results in reduced signal intensity, causing regions containing FNPs to appear darker in the images. As shown in Fig. 3e, the $T_2$ image of the seed coat reveals nearly complete signal quenching in the presence of FNPs, with a less pronounced reduction in the $T_2$ relaxation time observed in peeled seeds treated with FNPs compared to the control seed coat. These findings confirm that the majority of FNPs are localized on the seed coat. However, partial internalization of FNPs into the seed endosperm cannot be entirely ruled out.

### 3.4. Impact of FNPs-G on morphological and physiological parameters in cucumber plants

Seed germination rate and germination potential are the two most critical indicators for evaluating the germinative capacity of a seed and are essential for assessing seed vigor

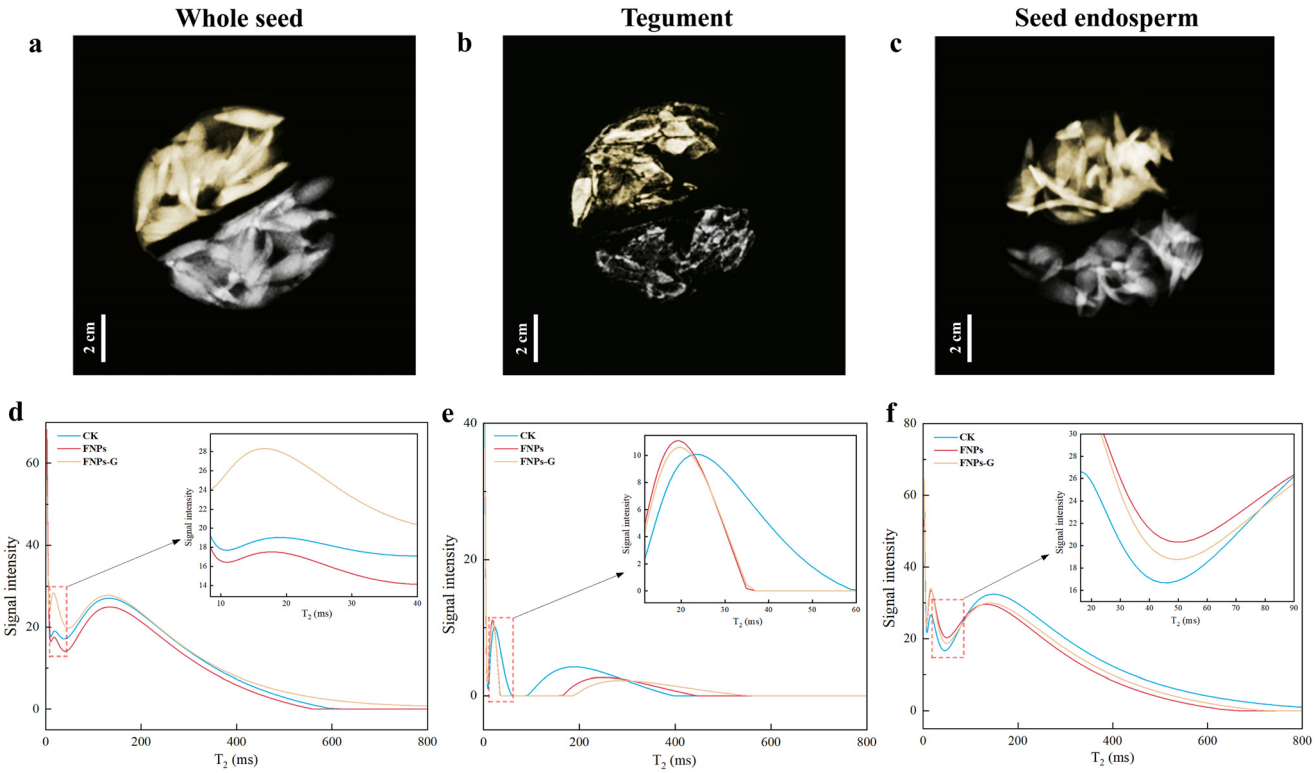


Fig. 3 (a–c) Representative 2D central axial sections of the whole seed, tegument, and seed endosperm, where the yellow markers represent control samples in the $T_2$ experiments. (d–f) Trend plots of signal intensity *versus* $T_2$ relaxation time (ms) for the seeds, seed coat, and seed endosperm after seed soaking with control, FNPs, and FNPs-G solutions, with insets showing the zoomed-in regions of the initial $T_2$ relaxation phase (0–40 ms).

and planting value.[32] In this study, immersion in a certain concentration of FNPs-G had no inhibitory effects on cucumber seed germination, suggesting that seed germinative ability was unaffected by exposure to nanoparticles. This further demonstrates the biosafety of FNPs (Fig. 4a). To more intuitively visualize the trends in cucumber seed germination and seedling growth, the number of germinated seeds was recorded daily over a 5-day period at different FNPs-G concentrations during a 16–48 h seed soaking interval. As depicted in Fig. 4b and c, compared with the control group, 200 mg $mL^{-1}$ FNPs-G substantially enhanced the germination and emergence rates of cucumber seeds, with the germination rate increasing by approximately 50%. This may be attributed to the PEG modification, which improved the hydrophilicity and biocompatibility of FNPs. This effect may have regulated the osmotic pressure within the seeds, thereby facilitating the uptake and utilization of nanoparticles, while promoting the softening of the seed coat and radicle breakthrough.

To verify whether FNPs possess ROS scavenging capability, the fluorescence intensity of the seeds after immersion was examined under a fluorescence microscope using DCFH-DA as the fluorescent probe (Fig. S2). The fluorescence images revealed that the fluorescence intensity of the seeds treated with FNPs-G was lower than that of the control group, suggesting that FNPs-G exerted a minimal effect on the oxidative stress response of the cells. Meanwhile, a comprehensive analysis in conjunction with ROS quantification data (Fig. 4d) demonstrated that compared to the CK treatment, FNPs-G immersion reduced the ROS content in the seeds by 13.9%, thus confirming the ROS-lowering ability of FNPs-G. When the pH or the concentration of $H_2O_2$ changes, FNPs-G can switch from a "producer" to a "scavenger".

As illustrated in Fig. 4e, FNPs-G not only enhanced the root length of the cucumber seedlings but also increased the number and density of root hairs relative to CK. By comparing the root lengths, the 200 mg $mL^{-1}$ FNPs-G treatment exhibited a significant advantage in promoting embryonic root growth, with an increase of approximately 7.2% compared to CK (Fig. 4f). Root vigor is a critical index for evaluating the physiological function and growth status of plant roots. FNPs-G treatment significantly enhanced the root vigor of the cucumber seedlings, with the 200 mg $mL^{-1}$ FNPs-G treatment increasing the root vigor by approximately 52.7% (Fig. 4g).

It is worth noting that the effects of seed nano-priming on the growth and development of cucumber plants have been scarcely investigated. However, some studies have reported that nanoparticles may exert toxic effects on soil organisms,[33] aquatic organisms,[34] and flying organisms,[35] in addition to potential phytotoxic effects on plants. This dual mechanism of action results in significant contradictions and complexity in the biological effects of nanoparticles within plant

 

a

| Treatments | Concentration (mg $L^{-1}$) | Germination rate (%) | Germination potential (%) |
|---|---|---|---|
| CK | 0 | 97.33±2.31a | 97.33±2.31a |
| FNPs-G | 50 | 97.33±2.31a | 97.33±2.31a |
| | 100 | 94.67±2.31a | 93.33±2.31a |
| | 200 | 98.67±2.31a | 98.67±2.31a |

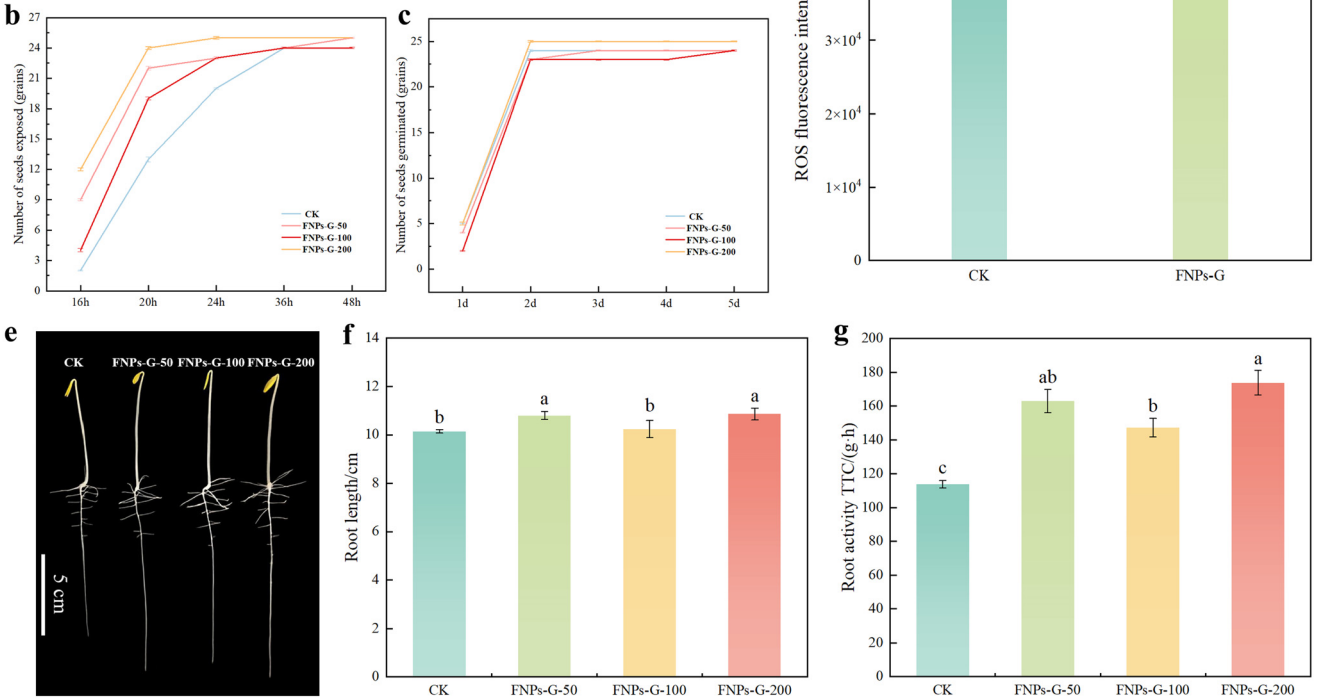


Fig. 4 Morphological and physiological analysis after the FNPs-G seed-soaking treatment. (a) Analysis of germination rate and germination potential of cucumbers after soaking seeds in CK and FNPs-G for 24 hours. The value is expressed as mean ± SD ($n$ = 3). (b and c) Trend of the number of exposed and germinated cucumber seeds changing over time. (d) ROS fluorescence intensity of seeds after 24 hours of treatment. (e) Representative images of cucumber seedlings on the 5th day of seed-soaking treatment with CK and different concentrations of FNPs-G. (f and g) Analysis of the root length and root viability of cucumbers by CK and different concentrations of FNPs-G. The images and charts shown represent at least three independent biological experiments. Statistical comparisons were conducted using univariate ANOVA. The letters denote statistical significance with respect to untreated seeds ($P \leq 0.05$).

systems, which are influenced by variations in plant species and nanoparticle properties. Treating seeds with 200 mg $mL^{-1}$ FNPs-G can effectively stimulate root growth and enhance vegetative growth in cucumber plants. Furthermore, nanoparticle-mediated seed priming has been documented to elicit stimulatory effects across various plant species.[36–39]

### 3.5. The modulatory effect of FNPs-G on morphological parameters of cucumbers under salt stress conditions

With 100 mM NaCl employed as the salt stress treatment, this study investigated whether treating seeds with 200 mg $mL^{-1}$ FNPs-G could mitigate the inhibitory effect of salt stress on cucumber seedling growth. The results demonstrated that FNPs-G enhance the salt tolerance of cucumber plants by increasing the activities of antioxidant enzymes, elevating the contents of soluble sugars and Pro, and reducing the levels of $H_2O_2$ and MDA (Fig. S3). Foliar spraying has been reported as a more effective approach,[40–42] but its efficiency may be compromised due to particle blockage at the leaf stomata when the concentration is excessively high. In prior investigations, it was observed that 50 mg $mL^{-1}$ FNPs-G also promoted the germination and early growth of cucumber seeds. Consequently, we further explored the effects of 50 mg $mL^{-1}$ FNPs-G foliar spray treatment on the growth and development of cucumber plants under salt stress, as well as its underlying mechanism for enhancing salt tolerance.

Under salt stress, the competitive interaction between $Na^+$ and $K^+$ during plant uptake results in excessive $Na^+$ accumulation, which not only impairs the absorption of $K^+$ and $Mg^{2+}$ but also disrupts the homeostasis of other mineral elements.[43] As illustrated in Table 1, compared with CK, 100 mM NaCl treatment led to a significant reduction in the concentrations of the nutrient elements $K^+$, $Ca^{2+}$, $Mg^{2+}$, $Fe^{2+}$, $P_2O_5$ and N in the cucumber leaves, while the concentration of $Na^+$ increased approximately 30-fold. This adverse situation was effectively mitigated by foliar application of FNPs-G. Specifically, the FNPs-G treatment not only provided supplemental nutritional support to the cucumber plants but also regulated the activity of ion channels or transporter proteins, thereby reducing the influx of $Na^+$ into the cells. This process not only alleviates the excessive accumulation of

**Table 1** Effects of different treatments on nutrient absorption in cucumber under salt stress, units in mg $mL^{-1}$

| Treatments | $Na^+$ | $K^+$ | $Ca^{2+}$ | $Mg^{2+}$ | $Fe^{2+}$ | $P_2O_5$ | N |
|---|---|---|---|---|---|---|---|
| CK | 132.11d | 4253.99a | 3605.29a | 984.91a | 14.81c | 1001.75a | 16.27a |
| NaCl | 3930.26a | 3625.38c | 1097.68d | 425.48d | 12.48d | 798.72c | 13.43b |
| N-50FG | 3476.54b | 4227.89a | 1561.61c | 527.19c | 80.82b | 732.15d | 15.51a |
| 200FG-N-50FG | 3071.35c | 4035.09b | 2573.10b | 769.01b | 85.73a | 821.05b | 15.77a |

$Na^+$ in the leaves but also establishes more optimal conditions for the uptake and accumulation of other essential nutrients (*e.g.*, $K^+$, $Ca^{2+}$, $Mg^{2+}$, *etc.*). Therefore, foliar spraying of FNPs-G regulates ion homeostasis, indirectly enhancing the uptake of other nutrients, thereby promoting cucumber growth and improving its salt tolerance. This balanced nutrient uptake plays a critical role in maintaining intracellular osmotic pressure, enzyme activity, and cellular structural integrity.

The treatment with 100 mM NaCl significantly decreased the chlorophyll content in the cucumber leaves, leading to leaf chlorosis, reduced photosynthetic capacity, and stunted plant growth. In contrast, the cucumber plants subjected to FNPs-G foliar spraying exhibited a markedly improved growth status under salt stress conditions. Compared with the NaCl treatment alone, the morphology of the cucumber leaves transitioned from yellowish to green, the plant height increased by 19.5%, and the dry and fresh weights of the leaves increased significantly by 19.3% and 21.1%, respectively. Additionally, the total leaf area expanded by 11.6% (as shown in Fig. 5). Compared with seed-soaking treatment, foliar spraying facilitates the rapid transfer of

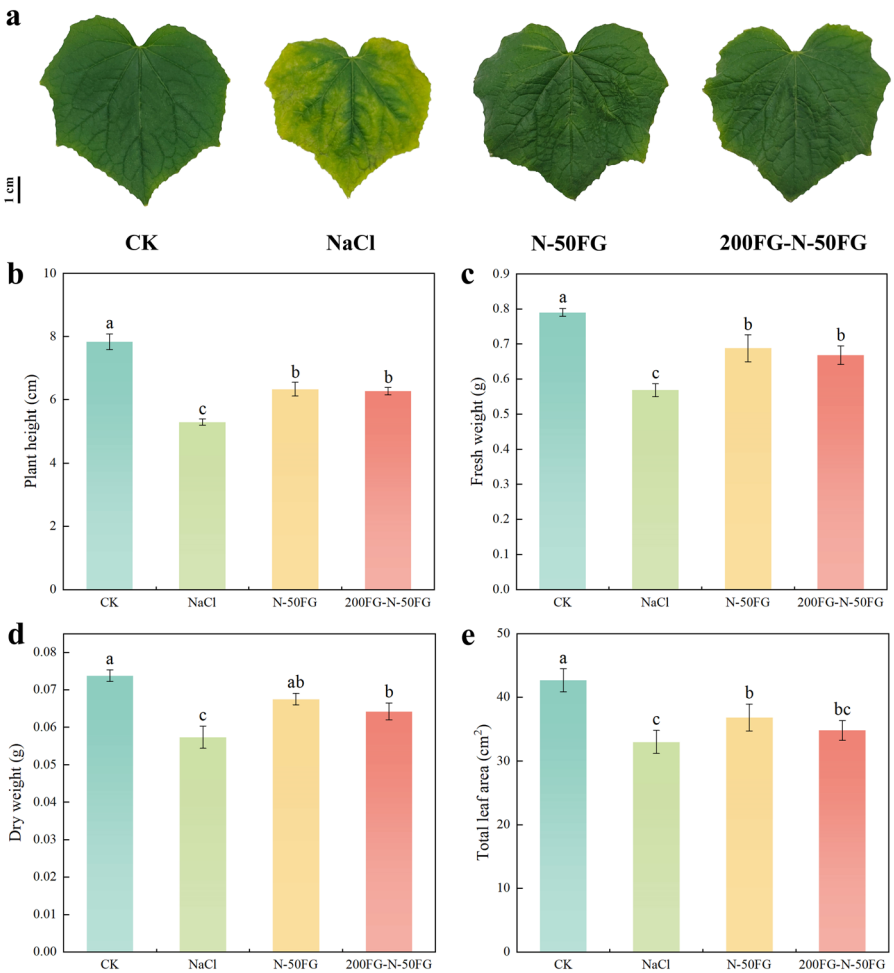


**Fig. 5** Effects of FNPs-G on the morphological indices and biomass of cucumber leaves under salt stress. (a) Representative images of cucumber leaves after treatment. (b–e) Effects of CK, NaCl, N-50FG and 200FG-N-50FG on the plant height, fresh weight, dry weight and total leaf area of cucumbers under salt stress. Among them, N-50FG was sprayed with 50 mg $mL^{-1}$ FNPs-G after salt stress treatment, and 200FG-N-50FG was grown to the three-leaf and one-heart stage after soaking seeds in 200 mg $mL^{-1}$ FNPs-G for 24 h, and then sprayed with 50 mg $mL^{-1}$ FNPs-G after salt stress treatment. The images and charts shown represent at least three independent biological experiments. Statistical comparisons were conducted using univariate ANOVA. The letters denote statistical significance with respect to untreated seeds ($P \leq 0.05$).

 

FNPs-G to the leaves and stems of the cucumber plants, enabling their absorption by the plant tissues and subsequent exertion of functional effects. This approach exhibits a more pronounced promoting effect. A study by He *et al.*[44] demonstrated that foliar application allows NMs to directly penetrate wheat leaves *via* stomata, resulting in higher accumulation levels and more efficient translocation within the plant. These findings are consistent with the results observed in the present experiment.

### 3.6. FNPs-G enhance antioxidant enzyme activity in cucumber under salt stress conditions

Salt stress induces a significant increase in ROS levels within cellular tissues, thereby directly triggering the activation of the antioxidant defense system in cucumber plants. This response serves to protect plant organelles and biomolecules under adverse environmental conditions.[5] In general, the antioxidant enzyme systems in plants work synergistically with non-enzymatic antioxidants to regulate ROS levels and

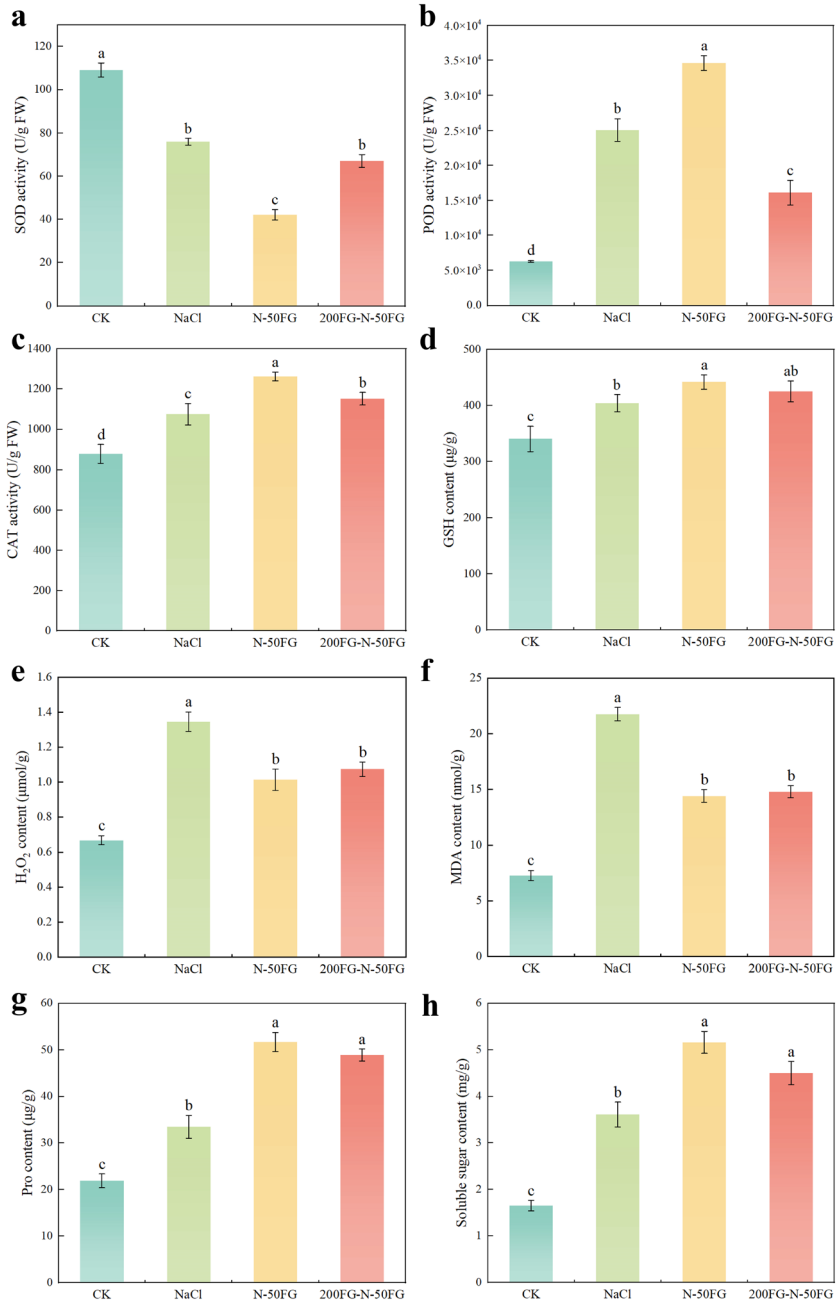


**Fig. 6** Effect of CK, NaCl, N-50FG and 200FG-N-50FG treatments on the (a) SOD activity; (b) POD activity; (c) CAT activity; (d) GSH content; (e) $H_2O_2$ content; (f) MDA content; (g) pro content and (h) soluble sugar content in cucumber leaves under salt stress. The charts shown represent at least three independent biological experiments. Statistical comparisons were conducted using univariate ANOVA. The letters denote statistical significance with respect to untreated seeds ($P \leq 0.05$).

maintain redox homeostasis. For instance, key antioxidant enzymes such as SOD, POD, and CAT play a critical role in sustaining ROS homeostasis and effectively protect plants from oxidative damage caused by excessive ROS production under salt stress conditions.[45,46] Fig. 6a indicates that under salt stress conditions, FNPs-G applied *via* foliar spraying were more efficiently absorbed and utilized by the cucumber leaves, resulting in a reduction in SOD activity through the direct scavenging of $O_2^{\bullet-}$ to decrease SOD substrates. Fig. 6b and c illustrate the changes in POD and CAT activities in the cucumber leaves under salt stress, respectively. Compared with NaCl treatment alone, foliar spraying of FNPs-G increased POD and CAT activities by 38% and 17.4%, respectively. Fig. 6d indicates that under salt stress, cucumber can promote the synthesis of glutathione through the synergistic effect of its intrinsic antioxidant enzyme system and the iron ions released by FNPs-G. In summary, FNPs-G foliar treatment enhances the ROS scavenging capacity of cucumber plants under salt stress by directly scavenging $O_2^{\bullet-}$. Additionally, our comparative analysis revealed that FNPs-G foliar spraying is more effective in scavenging ROS than the combined treatment of seed soaking followed by spraying.

### 3.7. The modulatory effect of FNPs-G on physiological parameters of cucumber plants under salt stress conditions

Compared with the CK treatment, NaCl significantly increased the levels of $H_2O_2$ and MDA in the cucumber leaves (Fig. 6e and f, respectively), primarily due to the excessive accumulation of ROS induced by salt stress in the cucumber plants. In contrast, foliar application of FNPs-G reduced the levels of $H_2O_2$ and MDA in the cucumber leaves by 24.6% and 33.8%, respectively, compared with NaCl treatment. The effects were 1.6- and 16.1-times that of the seed-soaking treatment (Fig. S3e and f), respectively, suggesting that foliar application of FNPs-G could facilitate their more efficient absorption and utilization by plants.

To maintain intracellular osmotic pressure balance under salt stress, the increased levels of Pro and soluble sugars in cucumber leaves contributed to activating the intracellular antioxidant defense system and alleviating salt stress-induced damage to cell membranes and other biomolecules. Compared with NaCl treatment, foliar application of FNPs-G increased the Pro content in the cucumber leaves by 54.6%, which was 6.6-times higher than that achieved by seed-soaking treatment (Fig. S3h). Additionally, the soluble sugar content in the foliar-sprayed FNPs-G treatment increased 3.13-fold compared with CK treatment and 1.43-fold compared with NaCl treatment. These results indicate that foliar spraying of FNPs-G more effectively promotes the accumulation of Pro and soluble sugars in cucumber leaves compared with FNPs-G seed-soaking treatment, thereby enhancing the tolerance of cucumber to salt stress. Notably, while N-50FG exhibits a slightly better performance in regulating cucumber salt tolerance than 200FG-N-50FG, no significant difference exists between these two treatments.

### 3.8. Comprehensive analysis of transcriptome characteristics

To gain a deeper understanding of the molecular mechanisms underlying FNPs-G regulation of salt tolerance in cucumber, we selected 16 samples from the CK, NaCl, N-50FG, and 200FG-N-50FG groups. Transcriptome data were analyzed *via* sequencing on the Illumina platform. The sequence numbers of the raw reads of the 16 samples ranged from 47958288–69965202, and the sequence numbers of the clean reads were between 43499668–63576750. Among them, the Q20 base proportion exceeded 97%, and the Q30 base proportion was greater than 93% (Table S1). Comparison of the quality-controlled, high-quality sequencing data with the reference genome of cucumber revealed that more than 96% of the sequencing data could be compared with the reference genome. This indicates that the sequencing data are of high quality and the comparison results are good, thus allowing further analysis.

By analyzing the differences in gene expression across different comparison groups, the potential mechanism through which FNPs-G enhance cucumber salt stress resistance was further elucidated. Based on the criteria of FDR $< 0.05$ and $|\log_2$ fold change$| \geq 1$, a total of 4873 differentially expressed genes (DEGs) were identified among the three pairwise comparisons: CK *vs.* NaCl, NaCl *vs.* N-50FG, and NaCl *vs.* 200FG-N-50FG. Among these DEGs, 2529 genes were upregulated, while 2344 genes were downregulated (Fig. S4a). To identify the key genes in FNPs-G that enhance cucumber salt tolerance, Venn diagrams were constructed to analyze the co-differentially expressed genes across the three comparison groups (Fig. S4b). The number of commonly differentially expressed genes shared among the three comparison groups was eight, including *CsaV4_5G002202* (purple acid phosphatase 17), *CsaV4_3G003796* (strigolactone esterase D14), *CsaV4_2G000442* (linoleate 9S-lipoxygenase 6), *CsaV4_4G000034* (hypothetical protein Csa_015018), *CsaV4_1G003513* (xylogen-like protein 11), *CsaV4_4G000246* (phenylalanine ammonia-lyase), *CsaV4_1G002454* (probable strigolactone esterase DAD2) and *CsaV4_5G003107* (repetitive proline-rich cell wall protein 1-like). These genes are highly likely to play crucial roles in FNPs-G-mediated alleviation of salt stress and regulation of growth and development in cucumbers.

To further elucidate the biological functions of the differentially expressed genes (DEGs), we mapped the annotated genes from the three comparison groups to terms in the Gene Ontology (GO) and Kyoto Encyclopedia of Genes and Genomes (KEGG) databases, aiming to identify significantly enriched genes associated with specific metabolic pathways. GO functional annotation and enrichment analysis were conducted on the DEGs across the

 

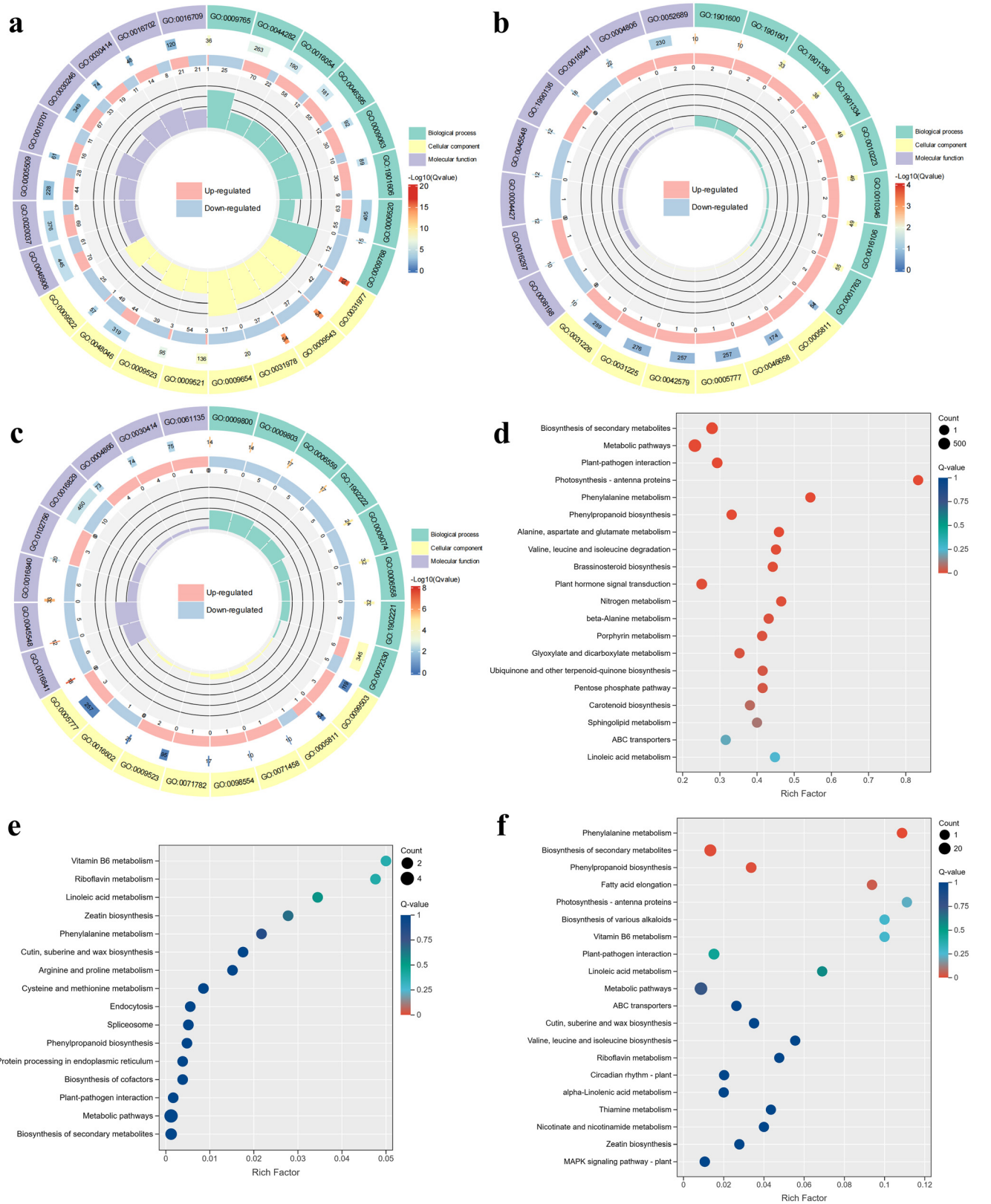


**Fig. 7** Effects of CK *vs.* NaCl, NaCl *vs.* N-50FG, and NaCl *vs.* 200FG-N-50FG on RNA sequencing analysis. (a–c) GO enrichment analysis of differential genes in the comparison groups of CK *vs.* NaCl, NaCl *vs.* N-50FG and NaCl *vs.* 200FG-N-50FG. (d–f) KEGG enrichment analysis of the comparison groups of CK *vs.* NaCl, NaCl *vs.* N-50FG and NaCl *vs.* 200FG-N-50FG.

three comparison groups, as illustrated in Fig. 7a–c, respectively. These genes are primarily enriched in three main categories: biological processes (BP), cellular components (CC), and molecular functions (MF). The differentially expressed genes in the CK *vs.* NaCl comparison group were mainly enriched in processes such as photosynthesis, transcriptional regulation, and amino acid catabolism in the BP category; in the CC category, they were mainly enriched in the photosystem, thylakoid, cell wall, and cell membrane; and in the MF category, they were mainly enriched in processes such as heme binding, enzyme modulator activity, and oxidoreductase activity. The GO annotation of differentially expressed genes in the NaCl *vs.* N-50FG comparison group was mainly enriched in the BP category in the processes of secondary metabolite biosynthesis and lactone biosynthesis; in the CC category, they were mainly enriched in peroxisome and plasma membrane components; and in the MF category, they were mainly enriched in iron-ion binding, hydrolase activity and oxidoreductase activity. The GO annotation of differentially expressed genes in the NaCl *vs.* 200FG-N-50FG comparison group was mainly enriched in the BP category in the processes of secondary metabolite synthesis and amino acid catabolism; in the CC category, the differentially expressed genes were mainly enriched in secretory vesicles, chloroplast membranes, and peroxisomes; in the MF category, the differentially expressed genes were mainly enriched in heme binding, iron ion binding, transferase activity, and lyase activity.

The top 20 metabolic pathways enriched in the KEGG analysis of the three comparison groups were selected, as illustrated in Fig. 7d–f, respectively. DEGs across the three comparison groups were highly enriched in pathways related to the biosynthesis of secondary metabolites, amino acids, and phenylpropanoids during metabolism. Additionally, differences were observed in pathways such as plant hormone signal transduction, MAPK signaling pathway, and plant–pathogen interaction. A detailed analysis of the top 20 enriched pathways was conducted. In the CK *vs.* NaCl comparison group, the most significantly enriched pathway for DEGs was photosynthetic antenna proteins, followed by phenylalanine metabolism and amino acid metabolism. Furthermore, enrichment was also observed in linoleic acid metabolism, as well as alanine, aspartate, and glutamate metabolism. In the NaCl *vs.* N-50FG comparison group, the most significantly enriched pathways among the DEGs included vitamin B6 metabolism, linoleic acid metabolism, phenylalanine metabolism, and arginine and proline metabolism. Additionally, enrichment was observed in zeatin biosynthesis and phenylalanine biosynthesis pathways. In the NaCl *vs.* 200FG-N-50FG comparison group, the most significantly enriched pathways among the DEGs were phenylalanine metabolism, photosynthetic antenna proteins, biosynthesis of various alkaloids, and vitamin B6 metabolism.

These results suggest that, upon exposure to salt stress, cucumbers may enhance their tolerance through the regulation of DEGs by accelerating key metabolic pathways such as secondary metabolite biosynthesis, amino acid metabolism, and photosynthesis. The activation of the phenylpropanoid biosynthesis pathway likely contributes to the synthesis of antioxidant substances (*e.g.*, phenolic compounds) and structural compounds (*e.g.*, lignin precursors), thereby strengthening the cell wall integrity and enhancing the plant antioxidant capacity, which is consistent with the reduced MDA and $H_2O_2$ levels observed in the FNPs-G-treated plants (Fig. 6e and f). Furthermore, the regulation of genes involved in plant-pathogen interactions may indicate that FNPs-G treatment enhances the immune response of cucumbers under salt stress, reduces pathogen invasion, and indirectly improves salt tolerance. In addition, enrichment of steroid biosynthesis pathways suggests potential regulation of membrane stability and ion permeability, which may contribute to the improved $Na^+/K^+$ homeostasis (Table 1). KEGG pathway maps highlighting differentially expressed genes in phenylpropanoid and steroid biosynthesis are presented in Fig. S15 (SI).

### 3.9. Comprehensive analysis of metabolome characteristics

Metabolites serve as the foundation of the phenotype of an organism and enable a more intuitive and effective understanding of biological processes and their underlying mechanisms. To comprehensively assess the overall metabolite differences among samples across groups and the variation within each group, principal component analysis (PCA) was performed on samples subjected to different treatments. As illustrated in Fig. S6a, the PCA results demonstrate that the data for CK, NaCl, N-50FG, and 200FG-N-50FG are dispersed, while the replicates within each group are tightly clustered. This aligns with experimental expectations and provides robust and reliable data support for subsequent theoretical analyses.

After detection using liquid chromatography-mass spectrometry (LC-MS), a total of 1359 metabolites were identified in cucumber leaves under four different treatment conditions (Fig. S6b). These metabolites can be broadly categorized into amino acids and their derivatives (23.69%), organic acids (13.76%), benzene and its substituted derivatives (10.89%), flavonoids (5.15%), terpenoids (4.86%), alkaloids (4.42%), and other types of compounds. Based on the volcano plot of differential metabolites (Fig. S5) and screening criteria of VIP $\geq$ 1, fold change $\geq$ 2, and fold change $\leq$ 0.5, a total of 3588 differential metabolites were identified across the three comparison groups: CK *vs.* NaCl, NaCl *vs.* N-50FG, and NaCl *vs.* 200FG-N-50FG. Among these differential metabolites, 1834 were upregulated and 1754 were downregulated. Through the screening and analysis of the Venn plot results for differential grouping, it was determined that there is a total of 135 overlapping differential metabolites among the three comparison groups, primarily consisting of amino acids and their derivatives, benzene and its derivatives, organic acids, alkaloids and others, followed by glycerophospholipids, flavonoids, terpenoids, heterocyclic compounds, lignans and coumarins.

 

Then, cluster analysis was conducted on the differential metabolites screened from the comparison groups of CK *vs.* NaCl, NaCl *vs.* N-50FG, and NaCl *vs.* 200FG-N-50FG (Fig. 8a–c, respectively), and the number of differential metabolites exhibited significant variation among these groups. By comparing the top 30 differential metabolites with marked differences across the three comparison groups, the results demonstrated that foliar application of FNPs-G significantly influenced the metabolic profile of cucumbers under salt stress. The primary metabolites included amino acids and their derivatives, terpenoids, heterocyclic compounds, benzene and its derivatives, and other compounds. Based on the identified differential metabolites, enrichment analysis was conducted on the KEGG pathway to further elucidate their functional roles.

As illustrated in Fig. 8d–f, in the CK *vs.* NaCl comparison group, a total of 66 differential metabolites were annotated to metabolic pathways. Among them, the most significantly enriched pathways included secondary metabolite biosynthesis, amino acid biosynthesis, alkaloid biosynthesis, and nucleotide metabolism. The top 20 pathways with significant differential metabolite enrichment were analyzed, and the most significantly enriched pathways were valine, leucine and isoleucine biosynthesis and degradation, and tryptophan metabolism. In the NaCl *vs.* N-50FG comparison group, a total of 40 differentially enriched metabolites were annotated to metabolic pathways, among which the most significantly enriched pathways included secondary metabolite biosynthesis and phenylalanine and tyrosine biosynthesis. The top 20 pathways with significantly different metabolite enrichment were analyzed. The most significant enrichment pathways were steroid biosynthesis and arginine biosynthesis. In the NaCl *vs.* 200FG-N-50FG comparison group, a total of 48 differential metabolites were annotated to metabolic pathways. The most significantly enriched pathways in this group included secondary metabolite biosynthesis, phenylalanine biosynthesis, carotenoid biosynthesis, and alkaloid biosynthesis. The top 20 pathways with significantly different metabolite enrichment were analyzed, and the most significant enrichment pathway was steroid biosynthesis.

### 3.10. Comprehensive analysis of transcriptome and metabolome

Biological processes are inherently complex and holistic in nature. Explaining complex biological processes and the regulation of biological networks solely based on single-omics data is challenging. Integrating multi-omics data for cross-validation can effectively reduce false positives arising from single-omics analyses. To further elucidate the effects of NaCl and FNPs-G under salt stress on gene expression and metabolite characteristics in cucumbers, a KEGG enrichment analysis bar chart was employed to analyze common pathways among the annotated differential gene KEGG pathways and metabolite KEGG pathways across different comparison groups (Fig. 9). Most co-enrichment pathways are related to the biosynthesis of secondary metabolites and

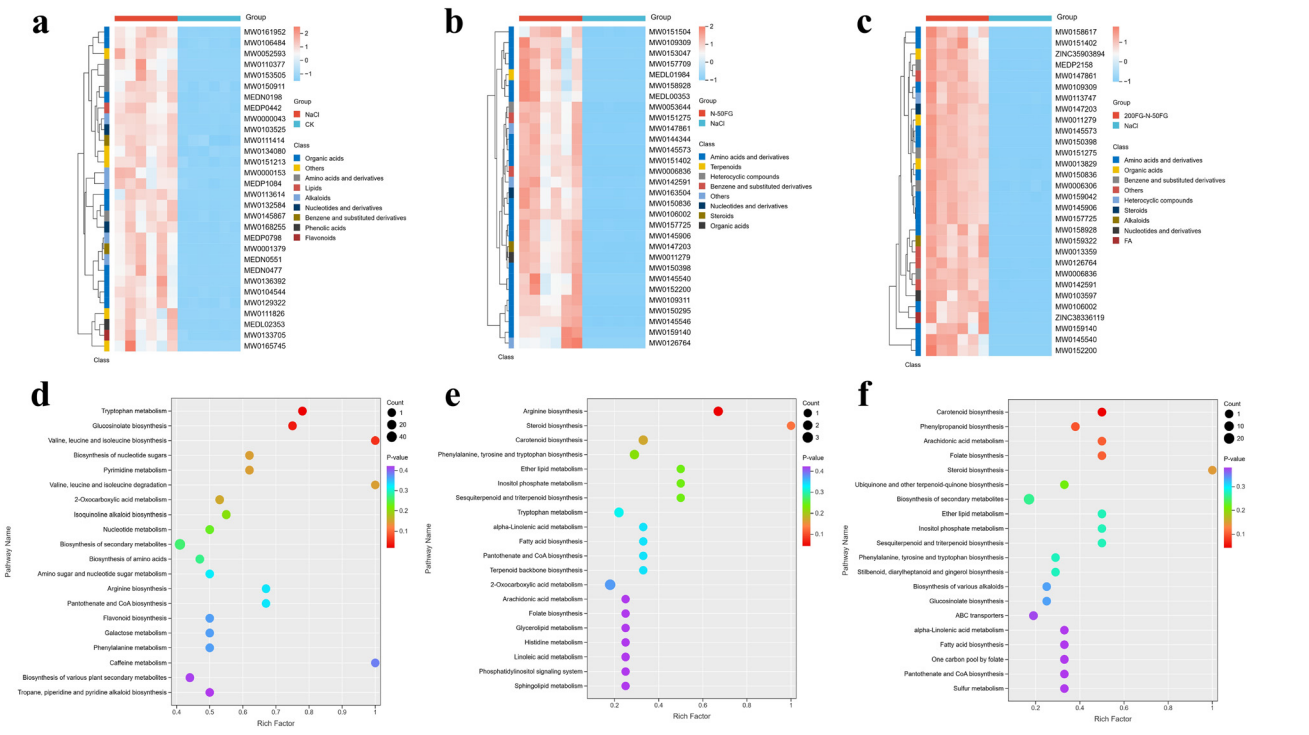


**Fig. 8** (a–c) Clustering heat maps of CK *vs.* NaCl, NaCl *vs.* N-50FG, and NaCl *vs.* 200FG-N-50FG. (d–f) KEGG enrichment point plots of CK *vs.* NaCl, NaCl *vs.* N-50FG, and NaCl *vs.* 200FG-N-50FG.

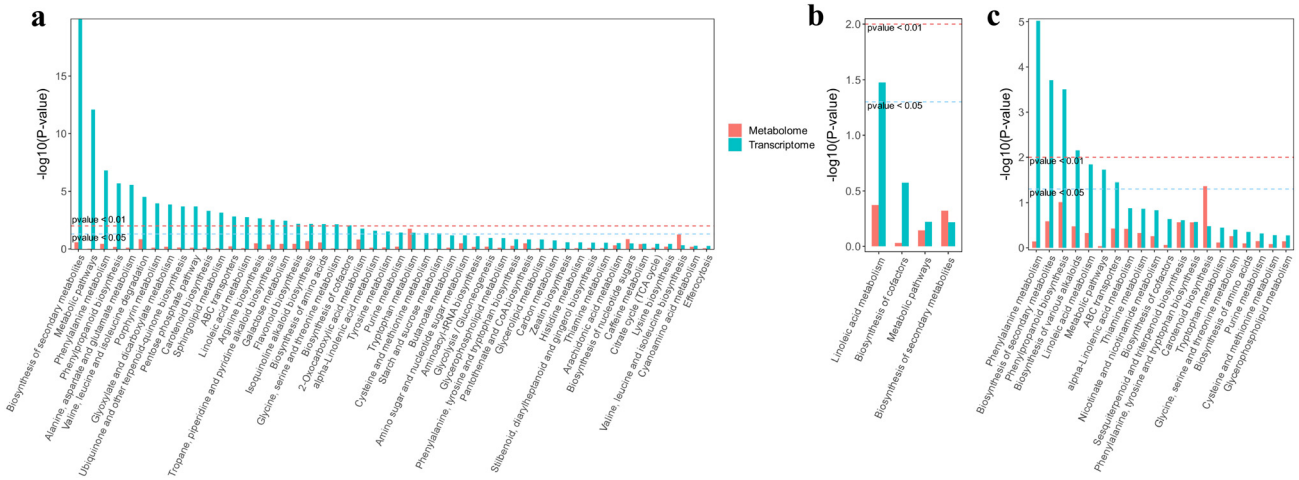


Fig. 9 KEGG common pathway analysis of differential genes and differential metabolites. (a) Overview of all enriched KEGG pathways, (b) top enriched pathways related to linoleic acid metabolism, (c) top enriched pathways related to phenylpropanoid biosynthesis.

amino acid metabolism, while the remaining metabolic pathways include linoleic acid metabolism, the biosynthesis of cofactors, and signal transduction. After foliar spraying of FNPs-G, the accumulation amounts of secondary metabolites such as organic acids, terpenoids, benzene and its derivatives, and alkaloids through biosynthesis were significantly higher than those treated with NaCl. Among these findings, foliar application of FNPs-G can further alleviate salt stress by enhancing phenylalanine metabolism, phenylpropanoid biosynthesis, and steroid biosynthesis, thereby improving the salt tolerance of cucumbers. In the amino acid metabolic pathway, foliar application of FNPs-G significantly promoted the biosynthesis of tyrosine and arginine in cucumbers while upregulating the gene expression of intracellular hydrolases and oxidoreductase. Meanwhile, tyrosine metabolites can effectively eliminate ROS that accumulate in cucumbers under salt stress conditions. This finding aligns with the results of this study, which demonstrate that foliar application of FNPs-G exhibits a significant advantage in ROS elimination compared to seed-soaking treatment (Fig. 10).

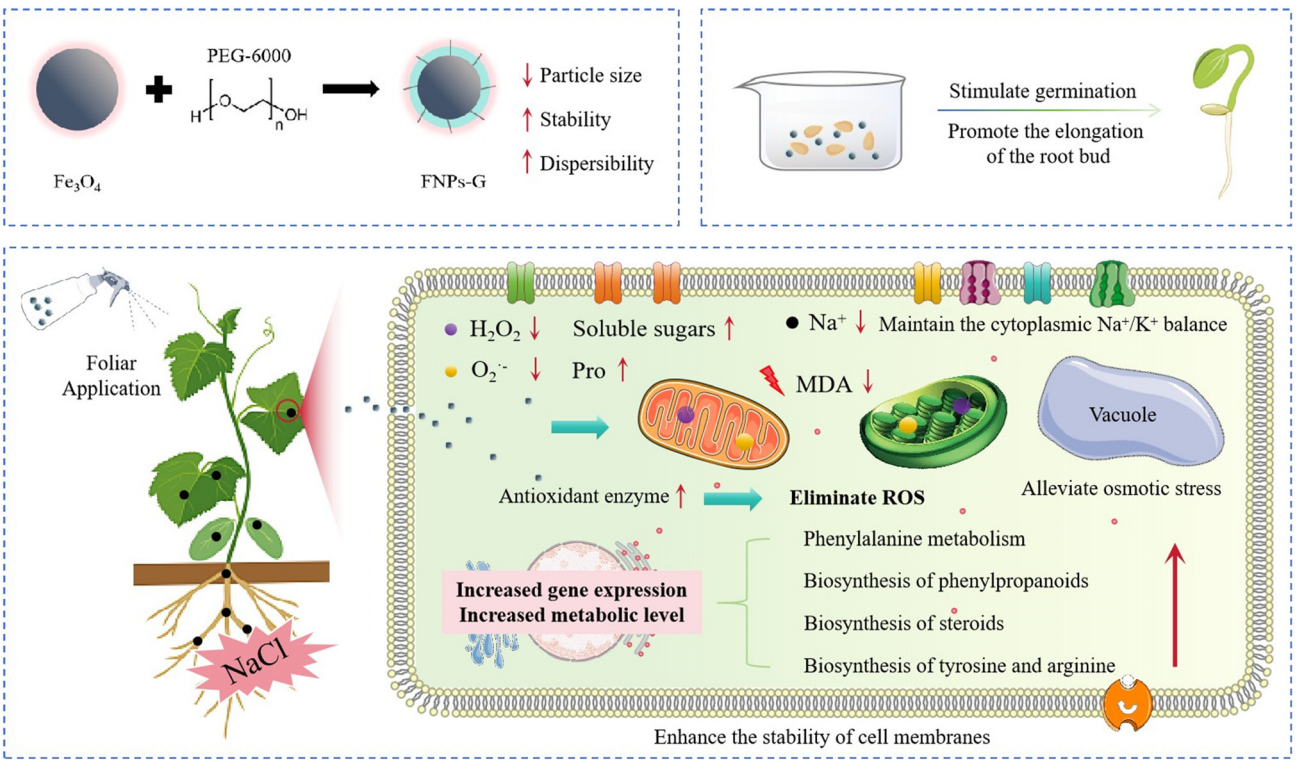


Fig. 10 Schematic of the experiment.

Under salt stress conditions, foliar application of FNPs-G can effectively activate or optimize key metabolic pathways, thereby enhancing the efficiency of secondary metabolite synthesis and strengthening the defense mechanisms of plants. Meanwhile, by regulating amino acid metabolism, FNPs-G ensure that plants maintain normal protein synthesis and cellular functions under salt stress, thus improving the salt tolerance of cucumber plants. Notably, comparative transcriptomic and metabolomic analysis revealed that the combined treatment (200FG-N-50FG, seed soaking followed by foliar spray) resulted in a greater enrichment of differentially expressed genes and metabolites than foliar spray alone (N-50FG). This suggests that FNPs-G treatment during the seed stage primes the plant's metabolism, leading to enhanced responses at later growth stages. Future research could explore seed nano-coating and seed nano-initiation techniques in greater depth, with the aim of gradually applying these methods to soil-based agricultural systems.

# 4. Discussion

Fe serves as a cofactor or activator for several key enzymes and proteins, playing a crucial role in maintaining redox homeostasis in plants.[13] $Fe_3O_4$ nanoparticles with intrinsic POD and CAT activities have been extensively verified and deeply studied. Their properties can effectively regulate the intracellular redox state, eliminate ROS accumulated in plants, and alleviate cell damage.[16] The modification of FNPs with PEG can substantially enhance their dispersion, stability, and biocompatibility in both aqueous and organic phases,[22,23] which is consistent with the results of this study.

Seed germination is a crucial stage in the life cycle of plants. In this study, after pre-treating cucumber seeds with FNPs-G, not only was particle dispersion observed inside the seeds, but also, compared to CK, 200 mg $mL^{-1}$ FNPs-G significantly increased the germination rate of cucumber seeds by approximately 50% (Fig. 4b). By comparing the root lengths, it was observed that the 200 mg $mL^{-1}$ FNPs-G treatment demonstrated a significant advantage in promoting root growth, increasing by approximately 7.2% compared to CK (Fig. 4f). This may be attributed to the PEG modification, which improved the hydrophilicity and biocompatibility of FNPs. This effect may have regulated the osmotic pressure within the seeds, thereby facilitating the uptake and utilization of nanoparticles, while promoting the softening of the seed coat and radicle breakthrough.

The damage caused by soil salinization to plants is obvious. In this study, NaCl significantly reduced the aboveground and root biomass of cucumbers. Fig. 5 illustrates the negative correlation between NaCl and the aboveground biomass. Under a 100 mM NaCl concentration, the application of FNPs-G by foliar spraying regulated the ion balance, indirectly promoting the absorption of other nutrients, increasing the above-ground biomass of cucumbers, and partially alleviating the negative effects of NaCl. ROS are by-products of plant aerobic metabolism, which are important signaling molecules that regulate biological developmental processes. Salt stress can induce homeostatic imbalance in cucumber plants, leading to a substantial accumulation of ROS, which disrupts normal metabolic processes, causes oxidative damage to plant cells, and may even trigger programmed cell death, thereby significantly affecting the growth and development of cucumber.[5,6] The fluorescence images (Fig. S2) showed that FNPs-G had little effect on the oxidative stress response of the cells. Furthermore, the comprehensive analysis based on the ROS quantitative data (Fig. 4d) indicates that the FNPs-G soaking treatment reduced the ROS content in the seeds by 13.9%. In general, the antioxidant enzyme systems in plants work synergistically with non-enzymatic antioxidants to regulate ROS levels and maintain redox homeostasis.[45,46] In this study, under salt stress conditions, FNPs-G applied *via* foliar spraying were more efficiently absorbed and utilized by cucumber leaves, resulting in a reduction in SOD activity through the direct scavenging of $O_2^{\bullet-}$ to decrease SOD substrates. Foliar spraying of FNPs-G increased the POD and CAT activities by 38% and 17.4%, respectively. Moreover, it significantly reduced the contents of $H_2O_2$ and MDA in cucumber leaves under salt stress (Fig. 6e and f, respectively). Therefore, FNPs-G may promote the development of plant cells and counteract the ROS inhibitory effect of NaCl on plant growth.

When plants perceive a harsh environment, stress adaptation involves not only antioxidant defense but also the maintenance of ionic and osmotic balance.[47] Under salt stress, excessive $Na^+$ accumulation and $K^+$ loss disrupt cellular ion equilibrium. In the present study, FNPs-G significantly reduced $Na^+$ accumulation (41%) and increased the $K^+$ levels (28%), thereby improving the $Na^+/K^+$ balance (Table 1). Similar ion-regulatory effects of nanomaterials under salt stress have been reported in other crop species.[48] Transcriptomic analysis further revealed significant enrichment of the steroid biosynthesis pathway (section 3.8), which is associated with membrane structure and stability under stress conditions and may contribute to improved ionic balance. In addition, FNPs-G markedly increased the proline (54.6%) and soluble sugar (3.13-fold) contents relative to NaCl treatment (Fig. 6g and h, respectively), consistent with previous reports on nanomaterial-induced osmoprotectant accumulation.[49] The coordinated transcriptional regulation of proline metabolism-related genes further supports enhanced osmotic adjustment capacity. Together with the antioxidant responses discussed above, these findings indicate that FNPs-G enhance salt tolerance through coordinated regulation of antioxidant defense, ion homeostasis, and osmotic adjustment.

Next, we employed transcriptomics and metabolomics techniques to gain a deeper understanding of the molecular mechanism by which FNPs-G regulate salt tolerance in cucumbers. The results of this study indicate that when cucumbers are subjected to salt stress, these differentially expressed genes may regulate salt stress by accelerating the synthesis of secondary metabolites, amino acid metabolism, and photosynthesis and other key metabolic pathways, thereby

enhancing the tolerance of cucumbers to salt stress (Fig. 7), which is similar to the research results reported by Wang *et al.*[50] After foliar spraying with FNPs-G, the accumulation of secondary metabolites such as organic acids, terpenoids, phenols and their derivatives, and alkaloids was significantly higher than that in the NaCl treatment group. Zhang *et al.*[51] conducted a study demonstrating that the phenylpropanoid pathway (including phenylpropanoid biosynthesis and phenylalanine metabolism) plays a significant role in controlling the response to salt stress. This finding is consistent with our transcriptomic data, which showed that the expression levels of phenylpropanoid biosynthesis genes were significantly higher in the FNPs-G-treated group (NaCl + foliar spray) than in the NaCl-only treatment group. This indicates that FNPs-G can further alleviate salt stress by enhancing phenylalanine metabolism and phenylpropanoid biosynthesis. Additionally, FNPs-G enhanced the biosynthesis of steroids in cucumber under salt stress through multiple pathways, which not only helps maintain normal cell functions but also may improve the salt tolerance in cucumber by regulating the hormone signaling and antioxidant systems. Besides the biosynthesis of secondary metabolites, differentially expressed genes and metabolites were also enriched in the metabolism of primary metabolites such as linoleic acid, which is consistent with the results from the study by Xu *et al.*[52]

Amino acid metabolism plays a significant and diverse role in the process by which plants respond to salt stress. Tyrosine is an important product in the phenylalanine metabolic pathway and serves as a precursor for the synthesis of some antioxidant substances. It is involved in the formation of various secondary metabolites, such as flavonoids and phenolic compounds. These compounds possess antioxidant properties and can eliminate ROS.[53] Arginine is an important nitrogen storage substance in plants. Under salt stress, arginine and its metabolites can help plants maintain the water balance within their cells by regulating osmotic pressure. Moreover, the polyamines and NO produced during arginine metabolism also participate in the antioxidant defense system of plants, eliminating ROS and alleviating oxidative damage caused by salt stress.[54] In this study, we found that foliar spraying of FNPs-G significantly promoted the biosynthesis of tyrosine and arginine in cucumber plants. At the same time, the metabolites of tyrosine could eliminate the ROS accumulated in cucumber plants due to salt stress. This is consistent with the significant advantage of foliar spraying of FNPs-G over the soaking treatment in removing ROS found in this experiment. Therefore, the changes in these secondary metabolite accumulations and related genes of free amino acids were significantly correlated with the enhancement in the salt tolerance level of cucumber by FNPs-G at the transcriptional and metabolic levels.

## 5. Conclusion

This study proposes a method that substantially enhances the germination rate of cucumber seeds and promotes seedling growth *via* FNPs-G, while scavenging ROS to improve the physiological indicators of growth in cucumbers and alleviate salt stress. FNPs-G, which exhibit antioxidant enzyme-like activities, can induce the up-regulation of defense-related gene expression, thereby enabling a rapid and robust defense response to adverse conditions. Gene expression and metabolic products primarily regulate salt stress responses by modulating the biosynthesis of secondary metabolites and amino acid metabolism, thereby enhancing the salt tolerance of cucumbers. In conclusion, FNPs-G serve as a type of nano-bio-stimulant that can be metaphorically regarded as a "vaccine" for plants. This acquired "vaccine" initiates and enhances the systemic defense mechanism, potentially alleviating damage to cucumber seedlings under various abiotic stresses. This approach may offer a sustainable solution to food security challenges posed by climate and environmental changes. In addition, the fate and environmental impact of the diffusion of FNPs-G in the soil–plant system remain a major concern and will be one of the main directions of our future research.

## Author contributions

Dan Xu & Bin Sheng: conceptualization, formal analysis, data curation, investigation, methodology, validation, writing – review & editing, writing – original draft. Zhi-Hao Lin: conceptualization, software, resources, investigation. Xiao-Bin Wen: conceptualization, investigation, validation. Xue-Ling Ye: conceptualization, resources, methodology. Zhi-Yong Liu: conceptualization, resources, supervision. Ge Chen: resources, visualization. Jun Lv: conceptualization, visualization. Dong-Hui Xu: conceptualization, resources, project administration, supervision, funding acquisition. Lin Qin: visualization, conceptualization. Xiao-Min Xu: visualization, conceptualization. Guang-Yang Liu: conceptualization, methodology, resources, funding acquisition, writing – review and editing, project administration, supervision.

## Conflicts of interest

The authors declare that there are no conflicts of interest.

## Data availability

Data will be available from the corresponding author upon reasonable request. Supplementary information (SI): detailed methods for POD activity detection, transcriptome analysis, and metabolome analysis (Texts S1–S3); supplementary figures (Fig. S1–S15) showing $Fe_3O_4$ NPs characterization (SEM/TEM, DLS, Zeta potential, FTIR, XRD, VSM), POD activity validation, ROS visualization, physiological parameters, transcriptomic and metabolomic analyses (PCA, volcano plots, KEGG enrichment), and KEGG pathway maps; supplementary tables (Tables S1–S3) summarizing sequencing data quality, salt concentration gradient test results, and correlation analysis of physiological parameters. See DOI: https://doi.org/10.1039/d5en00970g.

## Acknowledgements

The research was supported by the Basic Research Center, Innovation Program of Chinese Academy of Agricultural Sciences (CAAS-BRC-202612); the Beijing Natural Science Foundation (6242028); the National Key Research and Development Program of China (2022YFF0606800); the Special Fund for the Industrial System Construction of Modern Agriculture of China (CARS-23-E03); the Cross-Innovation Open Project of Food Flavor and Health, Beijing Technology & Business University; and the National Center of Technology Innovation for Comprehensive Utilization of Saline-Alkali (GYJ2023004).

## References

1 G. Sahbeni, M. Ngabire, P. K. Musyimi and B. Székely, Challenges and Opportunities in Remote Sensing for Soil Salinization Mapping and Monitoring: A Review, *Remote Sens.*, 2023, **15**(10), 2540, DOI: 10.3390/rs15102540.

2 I. B. Abdel-Farid, M. R. Marghany, M. M. Rowezek and M. G. Sheded, Effect of Salinity Stress on Growth and MetabolomicProfiling of Cucumis sativus and Solanum lycopersicum, *Plants*, 2020, **9**(11), 1626, DOI: 10.3390/plants9111626.

3 Y. Wang, N. Zafar, Q. Ali, H. Manghwar, G. Wang, L. Yu, X. Ding, F. Ding, N. Hong, G. Wang and S. Jin, CRISPR/Cas Genome Editing Technologies for Plant Improvement against Biotic and Abiotic Stresses: Advances, Limitations, and Future Perspectives, *Cell*, 2022, **11**(23), 3928, DOI: 10.3390/cells11233928.

4 B. Nowicka, J. Ciura, R. Szymańska and J. Kruk, Improving photosynthesis, plant productivity and abiotic stress tolerance – current trends and future perspectives, *J. Plant Physiol.*, 2018, **231**, 415–433, DOI: 10.1016/j.jplph.2018.10.022.

5 M. S. Kesawat, N. Satheesh, B. S. Kherawat, A. Kumar, H.-U. Kim, S.-M. Chung and M. Kumar, Regulation of Reactive Oxygen Species during Salt Stress in Plants and Their Crosstalk with Other Signaling Molecules-Current Perspectives and Future Directions, *Plants*, 2023, **12**(4), 864, DOI: 10.3390/plants12040864.

6 L. Zhao, T. Bai, H. Wei, J. L. Gardea-Torresdey, A. Keller and J. C. White, Nanobiotechnology-based strategies for enhanced crop stress resilience, *Nat. Food*, 2022, **3**, 829–836, DOI: 10.1038/s43016-022-00596-7.

7 X. Wen, Z. Lin, B. Sheng, X. Ye, Y. Zhao, G. Liu, G. Chen, L. Qin, X. Liu and D. Xu, Research Status of Agricultural Nanotechnology and Its Application in Horticultural Crops, *Nanomaterials*, 2025, **15**(10), 765, DOI: 10.3390/nano15100765.

8 Z. Lin, D. Xu, Y. Zhao, B. Sheng, Z. Wu, X. Wen, J. Zhou, G. Chen, J. Lv, J. Wang and G. Liu, Micro/Nanoplastics in plantation agricultural products: behavior process, phytotoxicity under biotic and abiotic stresses, and controlling strategies, *J. Nanobiotechnol.*, 2025, **23**, 231, DOI: 10.1186/s12951-025-03314-0.

9 L. Zhao, L. Lu, A. Wang, H. Zhang, M. Huang, H. Wu, B. Xing, Z. Wang and R. Ji, Nano-Biotechnology in Agriculture: Use of Nanomaterials to Promote Plant Growth and Stress Tolerance, *J. Agric. Food Chem.*, 2020, **68**(7), 1935–1947, DOI: 10.1021/acs.jafc.9b06615.

10 L. Lu, M. Huang, Y. Huang, P. F. X. Corvini, R. Ji and L. Zhao, Mn3O4 nanozymes boost endogenous antioxidant metabolites in cucumber (Cucumis sativus) plant and enhance resistance to salinity stress, *Environ. Sci.: Nano*, 2020, **7**, 1692–1703, DOI: 10.1039/d0en00214c.

11 K. A. Abdullah, T. F. Tahir, A. F. Qader, R. A. Omer and K. A. Othman, Nanozymes: Classification and Analytical Applications – A Review, *J. Fluoresc.*, 2024, **35**(7), 1–15, DOI: 10.1007/s10895-024-03930-3.

12 M. N. Khan, Y. Li, C. Fu, J. Hu, L. Chen, J. Yan, Z. Khan, H. Wu and Z. Li, CeO2 Nanoparticles Seed Priming Increases Salicylic Acid Level and ROS Scavenging Ability to Improve Rapeseed Salt Tolerance, *Glob. Chall.*, 2022, **6**(7), 2200025, DOI: 10.1002/gch2.202200025.

13 L. Junlin, X. Sophia, W. Nan, S. Zhongyue, T. Lina, Z. Guojun, T. John, Z. Yulin, S. Yujie and C. Shaowei, Iron nanoparticle/carbon nanotube composite as oxidase-like nanozyme for visual analysis of total antioxidant capacity, *Food Chem.: X*, 2024, **25**, 102093, DOI: 10.1016/j.fochx.2024.102093.

14 G. Lizeng, Z. Jie, N. Leng, Z. Jinbin, Z. Yu, G. Ning, W. Taihong, F. Jing, Y. Dongling, P. Sarah and Y. Xiyun, Intrinsic peroxidase-like activity of ferromagnetic nanoparticles, *Nat. Nanotechnol.*, 2007, **2**(9), 577–583, DOI: 10.1038/nnano.2007.260.

15 M. Ebadi, A. Rifqi Md Zain, T. H. Tengku Abdul Aziz, H. Mohammadi, C. A. T. Tee and M. Rahimi Yusop, Formulation and Characterization of Fe3O4@PEG Nanoparticles Loaded Sorafenib; Molecular Studies and Evaluation of Cytotoxicity in Liver Cancer Cell Lines, *Polymers*, 2023, **15**(4), 971, DOI: 10.3390/POLYM15040971.

16 M. Xie, F. Li, Y. Li, K. Qian, Y. Liang, B. Lei, Y. Liu, J. Cui and Y. Xiao, Iron-doped carbon dots nanozyme scavenged reactive oxygen species system for inhibiting effectively the uptake of arsenic in lettuce, *Chem. Eng. J.*, 2025, **506**, 159956, DOI: 10.1016/j.cej.2025.159956.

17 H. Dong, W. Du, J. Dong, R. Che, F. Kong, W. Cheng, M. Ma, N. Gu and Y. Zhang, Depletable peroxidase-like activity of Fe3O4 nanozymes accompanied with separate migration of electrons and iron ions, *Nat. Commun.*, 2022, **13**, 5365, DOI: 10.1038/s41467-022-33098-y.

18 M. Rui, C. Ma, Y. Hao, J. Guo, Y. Rui, X. Tang, Q. Zhao, X. Fan, Z. Zhang, T. Hou and S. Zhu, Iron Oxide Nanoparticles as a Potential Iron Fertilizer for Peanut (Arachis hypogaea), *Front. Plant Sci.*, 2016, **7**, 815, DOI: 10.3389/fpls.2016.00815.

19 L. Meijie, W. Shunsuke, G. Fei and D. Christian, Iron Nutrition in Plants: Towards a New Paradigm?, *Plants*, 2023, **12**(2), 384–384, DOI: 10.3390/plants12020384.

20 B. S. Shirani, S. Paolo and V. Josh, Iron oxide (Fe2O3) nanoparticles alleviate PEG-simulated drought stress in grape (Vitis vinifera L.) plants by regulating leaf

antioxidants, *Sci. Hortic.*, 2023, **312**, 111847, DOI: 10.1016/j.Scienta.2023.111847.

21 C. Zapata-Hernandez, G. Durango-Giraldo, D. López, R. Buitrago-Sierra and K. Cacua, Surfactants versus surface functionalization to improve the stability of graphene nanofluids, *J. Dispersion Sci. Technol.*, 2021, **43**(11), 1717–1724, DOI: 10.1080/01932691.2021.1880429.

22 Y. Zhang, J. Duan, R. Liu, E. Petropoulos, Y. Feng, L. Xue, L. Yang and S. He, Efficient magnetic capture of PE microplastic from water by PEG modified Fe3O4 nanoparticles: Performance, kinetics, isotherms and influence factors, *J. Environ. Sci.*, 2023, **147**, 677–687, DOI: 10.1016/j.jes.2023.07.025.

23 Z. Deng, Y. Luo, M. Bian, X. Guo and N. Zhang, Synthesis of easily renewable and recoverable magnetic PEI-modified Fe3O4 nanoparticles and its application for adsorption and enrichment of tungsten from aqueous solutions, *Environ. Pollut.*, 2023, **330**, 121703, DOI: 10.1016/j.envpol.2023.121703.

24 G. Antarnusa, P. D. Jayanti, Y. R. Denny and A. Suherman, Utilization of co-precipitation method on synthesis of Fe3O4/PEG with different concentrations of PEG for biosensor applications, *Materialia*, 2022, **25**, 101525, DOI: 10.1016/j.mtla.2022.101525.

25 S. M. Youssef, S. A. Abd Elhady, R. M. Aref and G. S. Riad, Salicylic Acid Attenuates the Adverse Effects of Salinity on Growth and Yield and Enhances Peroxidase Isozymes Expression more Competently than Proline and Glycine Betaine in Cucumber Plants, *Gesunde Pflanz.*, 2018, **70**, 75–90, DOI: 10.1007/s10343-017-0413-9.

26 N. J. Langenfeld and B. Bugbee, Germination and seedling establishment for hydroponics: The benefit of slant boards, *PLoS One*, 2022, **17**(10), e0275710, DOI: 10.1371/journal.pone.0275710.

27 K. M. Salikhov, Similarities and Differences in the Effect of Dipole–Dipole and Exchange Interactions on the Shape of the EPR Spectrum of Dilute Solutions of Paramagnetic Particles, *Appl. Magn. Reson.*, 2024, **55**, 1587–1603, DOI: 10.1007/s00723-024-01647-x.

28 D.-L. Zhao, P. Teng, Y. Xu, Q.-S. Xia and J.-T. Tang, Magnetic and inductive heating properties of Fe3O4/polyethylene glycol composite nanoparticles with core–shell structure, *J. Alloys Compd.*, 2010, **502**, 392–395, DOI: 10.1016/j.jallcom.2010.04.177.

29 X. Wang, A. Deng, W. Cao, Q. Li, L. Wang, J. Zhou, B. Hu and X. Xing, Synthesis of chitosan/poly (ethylene glycol)-modified magnetic nanoparticles for antibiotic delivery and their enhanced anti-biofilm activity in the presence of magnetic field, *J. Mater. Sci.*, 2018, **53**, 6433–6449, DOI: 10.1007/s10853-018-1998-9.

30 C. He, S. Wu, N. Zhao, C. Shi, E. Liu and J. Li, Carbon-Encapsulated Fe3O4 Nanoparticles as a High-Rate Lithium Ion Battery Anode Material, *ACS Nano*, 2013, **7**(5), 4459–4469, DOI: 10.1021/nn401059h.

31 E. A. Setiadi, P. Sebayang, M. Ginting, A. Y. Sari, C. Kurniawan, C. S. Saragih and P. Simamora, The synthesization of Fe3O4 magnetic nanoparticles based on natural iron sand by co-precipitation method for the used of the adsorption of Cu and Pb ions, *J. Phys.: Conf. Ser.*, 2016, **776**, 012020, DOI: 10.1088/1742-6596/776/1/012020.

32 W. M. Waterworth, C. M. Bray and C. E. West, The importance of safeguarding genome integrity in germination and seed longevity, *J. Exp. Bot.*, 2015, **66**(12), 3549–3558, DOI: 10.1093/jxb/erv080.

33 Y. Ding, J.-T. Zheng, Y.-N. Wang, D. Wu and D. Zhu, Presence of microplastics enhanced the toxicity of silver nanoparticles on the collembolan Folsomia candida, *Chemosphere*, 2024, **366**, 143557, DOI: 10.1016/j.chemosphere.2024.143557.

34 Z. Liu, C. R. Malinowski and M. S. Sepúlveda, Emerging trends in nanoparticle toxicity and the significance of using Daphnia as a model organism, *Chemosphere*, 2021, **291**, 132941, DOI: 10.1016/j.chemosphere.2021.132941.

35 G. Glavan, T. Milivojević, J. Božič, K. Sepčić and D. Drobne, Feeding Preference and Sub-chronic Effects of ZnO Nanomaterials in Honey Bees (Apis mellifera carnica), *Arch. Environ. Contam. Toxicol.*, 2017, **72**, 471–480, DOI: 10.1007/s00244-017-0385-x.

36 N. S. H. B. H. Zaim, H. L. Tan, S. M. A. Rahman, N. F. Abu Bakar, M. S. Osman, V. K. Thakur and N. Radacsi, Recent Advances in Seed Coating Treatment Using Nanoparticles and Nanofibers for Enhanced Seed Germination and Protection, *J. Plant Growth Regul.*, 2023, **42**, 7374–7402, DOI: 10.1007/s00344-023-11038-4.

37 N. Yan, J. Cao, J. Wang, X. Zou, X. Yu, X. Zhang and T. Si, Seed priming with graphene oxide improves salinity tolerance and increases productivity of peanut through modulating multiple physiological processes, *J. Nanobiotechnol.*, 2024, **22**, 565, DOI: 10.1186/s12951-024-02832-7.

38 M. Tondey, A. Kalia, A. Singh, G. S. Dheri, M. S. Taggar, E. Nepovimova, O. Krejcar and K. Kuca, Seed Priming and Coating by Nano-Scale Zinc Oxide Particles Improved Vegetative Growth, Yield and Quality of Fodder Maize (Zea mays), *Agronomy*, 2021, **11**(4), 729, DOI: 10.3390/agronomy11040729.

39 K. Zhang, Z. Khan, Q. Yu, Z. Qu, J. Liu, T. Luo, K. Zhu, J. Bi, L. Hu and L. Luo, Biochar Coating Is a Sustainable and Economical Approach to Promote Seed Coating Technology, Seed Germination, Plant Performance, and Soil Health, *Plants*, 2022, **11**(21), 2864, DOI: 10.3390/plants11212864.

40 L. Wei, L. Ji, C. Rico, C. He, I. Shakoor, M. Fakunle, X. Lu, Y. Xia, Y. Hou and J. Hong, Transcriptomics Reveals the Pathway for Increasing Brassica chinensis L. Yield under Foliar Application of Titanium Oxide Nanoparticles, *J. Agric. Food Chem.*, 2024, **72**(34), 18957–18970, DOI: 10.1021/acs.jafc.4c04075.

41 X. Cao, L. Yue, C. Wang, X. Luo, C. Zhang, X. Zhao, F. Wu, J. C. White, Z. Wang and B. Xing, Foliar Application with Iron Oxide Nanomaterials Stimulate Nitrogen Fixation, Yield, and Nutritional Quality of Soybean, *ACS Nano*, 2022, **16**(1), 1170–1181, DOI: 10.1021/acsnano.1c08977.

42 J. M. Cantu, Y. Ye, J. A. Hernandez-Viezcas, N. Zuverza-Mena, J. C. White and J. L. Gardea-Torresdey, Tomato Fruit

Nutritional Quality Is Altered by the Foliar Application of Various Metal Oxide Nanomaterials, *Nanomaterials*, 2022, **12**(14), 2349, DOI: 10.3390/nano12142349.

43 M. J. Hassan, M. Zhou, Y. Ling and Z. Li, Diethyl aminoethyl hexanoate ameliorates salt tolerance associated with ion transport, osmotic adjustment, and metabolite reprograming in white clover, *BMC Plant Biol.*, 2024, **24**, 950, DOI: 10.1186/s12870-024-05657-6.

44 C. He, T. Wu, J. Li, X. Zhang, Z. Zheng, Y. Gao, C. Zhang, T. Zhong, Y. Zhang and F. Du, Bio-stimulant based nanodelivery system for pesticides with high adhesion and growth stimulation, *Chem. Eng. J.*, 2024, **491**, 151904, DOI: 10.1016/j.cej.2024.151904.

45 P. Dvořák, Y. Krasylenko, A. Zeiner, J. Šamaj and T. Takáč, Signaling Toward Reactive Oxygen Species-Scavenging Enzymes in Plants, *Front. Plant Sci.*, 2020, **11**, 618835, DOI: 10.3389/fpls.2020.618835.

46 H. V. Ranjith, D. Sagar, V. K. Kalia, A. Dahuja and S. Subramanian, Differential Activities of Antioxidant Enzymes, Superoxide Dismutase, Peroxidase, and Catalase vis-à-vis Phosphine Resistance in Field Populations of Lesser Grain Borer (Rhyzopertha dominica) from India, *Antioxidants*, 2023, **12**(2), 270, DOI: 10.3390/antiox12020270.

47 G. Tripathi, S. Dutta, A. Mishra, S. Basu, V. Gupta and C. Kamaraj, Nanomaterials impact in phytohormone signaling networks of plants – A critical review, *Plant Sci.*, 2024, **352**, 112373, DOI: 10.1016/j.plantsci.2024.112373.

48 L. Rossi, W. Zhang, A. P. Schwab and X. Ma, Uptake, Accumulation, and in Planta Distribution of Coexisting Cerium Oxide Nanoparticles and Cadmium in Glycine max (L.) Merr, *Environ. Sci. Technol.*, 2017, **51**(21), 12815–12824, DOI: 10.1021/acs.est.7b03363.

49 A. Aslam, Z. Noreen, M. Rashid, M. Aslam, T. Hussain, A. Younas, S. Fiaz, K. A. Attia and A. A. Mohammed, Understanding the role of magnetic (Fe3O4) nanoparticle to mitigate cadmium stress in radish (Raphanus sativus L.), *Bot. Stud.*, 2024, **65**, 20, DOI: 10.1186/s40529-024-00420-4.

50 H. Wang, C. Hao, L. Chen and D. Liu, Comparative physiological and transcriptomic analyses reveal enhanced mitigation of cadmium stress in peanut by combined Fe3O4/ZnO nanoparticles, *J. Hazard. Mater.*, 2025, **489**, 137931, DOI: 10.1016/j.jhazmat.2025.137931.

51 Q. Zhang, S. Wang, B. Qin, H. y. Sun, X. k. Yuan, Q. Wang, J. Xu, Z. Yin, Y. l. Du, J. d. Du and C. Li, Analysis of the transcriptome and metabolome reveals phenylpropanoid mechanism in common bean (Phaseolus vulgaris) responding to salt stress at sprout stage, *Food Energy Secur.*, 2023, **12**(5), 481, DOI: 10.1002/fes3.481.

52 H. Xu, N. G. Halford, G. Guo, Z. Chen, Y. Li, L. Zhou, C. Liu and R. Xu, Transcriptomic and Metabolomic Analyses Reveal the Importance of Lipid Metabolism and Photosynthesis Regulation in High Salinity Tolerance in Barley (Hordeum vulgare L.) Leaves Derived from Mutagenesis Combined with Microspore Culture, *Int. J. Mol. Sci.*, 2023, **24**(23), 16757, DOI: 10.3390/ijms242316757.

53 Y. Sun, Y. Zhou, Q. Long, J. Xing, P. Guo, Y. Liu, C. Zhang, Y. Zhang, A. R. Fernie, Y. Shi, Y. Luo, J. Luo and C. Jin, OsBCAT2, a gene responsible for the degradation of branched-chain amino acids, positively regulates salt tolerance by promoting the synthesis of vitamin B5, *New Phytol.*, 2024, **241**(6), 2558–2574, DOI: 10.1111/nph.19551.

54 N. Napieraj, M. Reda and M. Janicka, The role of NO in plant response to salt stress: interactions with polyamines, *Funct. Plant Biol.*, 2020, **47**(10), 865–879, DOI: 10.1071/fp19047.